(12) INTERNATIONAL APPLICATION PUBLISHED UNDER THE PATENT COOPERATION TREATY (PCT)

(19) World Intellectual Property Organization
International Bureau

(43) International Publication Date
8 November 2001 (08.11.2001)

PCT

(10) International Publication Number
WO 01/83482 A1

(51) International Patent Classification[7]: C07D 471/04, 471/08, 487/04, 487/08, C07F 1/08, 1/10, 3/06, 15/02

(21) International Application Number: PCT/US01/14374

(22) International Filing Date: 3 May 2001 (03.05.2001)

(25) Filing Language: English

(26) Publication Language: English

(30) Priority Data:
60/201,543 3 May 2000 (03.05.2000) US

(71) Applicant *(for all designated States except US)*: **THE SCRIPPS RESEARCH INSTITUTE** [US/US]; 10550 North Torrey Pines Road, La Jolla, CA 92037 (US).

(72) Inventor; and

(75) Inventor/Applicant *(for US only)*: **BOGER, Dale, L.** [US/US]; 2819 Via Posada, La Jolla, CA 92037 (US).

(74) Agents: **LEWIS, Donald, G.** et al.; The Scripps Research Institute, 10550 North Torrey Pines Road, TPC-8, La Jolla, CA 92037 (US).

(81) Designated States *(national)*: AE, AG, AL, AM, AT, AU, AZ, BA, BB, BG, BR, BY, BZ, CA, CH, CN, CR, CU, CZ, DE, DK, DM, DZ, EE, ES, FI, GB, GD, GE, GH, GM, HR, HU, ID, IL, IN, IS, JP, KE, KG, KP, KR, KZ, LC, LK, LR, LS, LT, LU, LV, MA, MD, MG, MK, MN, MW, MX, MZ, NO, NZ, PL, PT, RO, RU, SD, SE, SG, SI, SK, SL, TJ, TM, TR, TT, TZ, UA, UG, US, UZ, VN, YU, ZA, ZW.

(84) Designated States *(regional)*: ARIPO patent (GH, GM, KE, LS, MW, MZ, SD, SL, SZ, TZ, UG, ZW), Eurasian patent (AM, AZ, BY, KG, KZ, MD, RU, TJ, TM), European patent (AT, BE, CH, CY, DE, DK, ES, FI, FR, GB, GR, IE, IT, LU, MC, NL, PT, SE, TR), OAPI patent (BF, BJ, CF, CG, CI, CM, GA, GN, GW, ML, MR, NE, SN, TD, TG).

Published:
— *with international search report*

For two-letter codes and other abbreviations, refer to the "Guidance Notes on Codes and Abbreviations" appearing at the beginning of each regular issue of the PCT Gazette.

(54) Title: DNA ALKYLATING AGENT AND ACTIVATION THEREOF

(57) Abstract: N^2-derivatives of methyl 1,2,9,9a-tetrahydrocyclopropa[c]pyrido[3,2-e]indol-4-one-7-carboxylate (CPyI) were synthesized and shown to have DNA alkylation activity and cytotoxic activity that is susceptible to catalysis by metal ions, including Zn^{2+}. This activation promotes DNA minor groove adenine N3 alkylation in a manner analogous to that of CC-1065 and the duocarmycins, and represents a new means of *in situ* activation for this class of DNA alkylating agent.

WO 01/83482 A1

DNA ALKYLATING AGENT AND ACTIVATION THEREOF

Description

Technical Field:

The invention relates to DNA alkylating agents and to processes for their activation and use *in situ*. More particularly, the invention relates to DNA alkylating agents having a methyl 1,2,9,9a-tetrahydrocyclopropa[c]pyrido [3,2-e]indol-4-one-7-carboxylate (CPyI) head group and to catalytic processes for their metal cation complexation, activation, and use as DNA alkylating agents and cytotoxic agents.

Background:

Several well established methods have been discovered or developed for selective activation of DNA binding agents which initiate reactivity toward DNA including reductive activation (mitomycins), oxidative activation (aflatoxin), disulfide or trisulfide cleavage (calicheamicin), photochemical activation (psoralen), and oxidant activation of metal complexes (bleomycin), e.g., see D. S. Johnson, et al., In *Comprehensive Supramolecular Chemistry*; Lehn, J. M., Ed., Pergamon: Oxford, 1996, Vol. 4, Chapter 3, pp 73-176; and, more generally, *Molecular Aspects of Anticancer Drug-DNA Interactions*; S. Neidle, et al., Eds.; CRC: Boca Raton, 1993 and 1994; Vol. 1 and 2. Many of these have been exploited in the development of therapeutics to impart selective activity against tumor cells or to provide a means to effect and control reactivity towards DNA for use as research tools (e.g., synthetic nucleases).

(+)-Duocarmycin SA (DSA, **1**) is a remarkably potent antitumor antibiotic (IC_{50} = 10 pM, L1210) disclosed in 1990 (Ichimura, M.; et al. *J. Antibiot.* **1990**, *43*, 1037; Ichimura, M.; et al. *J. Antibiot.* **1991**, *44*, 1045) that has been shown to selectively bind and alkylate DNA (Figure 1) (Boger, D. L.; et al. *J. Am. Chem. Soc.* **1993**, *115*, 9025). (+)-Duocarmycin SA exhibits enhanced stability and corresponding biological potency compared to its predecessors, (+)-duocarmycin

A (DA, **2**) (Ohba, K.; et al. *J. Antibiot.* **1988**, *41*, 1515; Takahashi, I.; et al. *J. Antibiot.* **1988**, *41*, 1915; Yasuzawa, T.; et al. *Chem. Pharm. Bull.* **1988**, *36*, 3728; Ichimura, M.; et al. *J. Antibiot.* **1988**, *41*, 1285; Ishii, S.; et al. *J. Antibiot.* **1989**, *42*, 1713) and (+)-CC-1065 (**3**) (Hanka, L. J.; et al. *J. Antibiot.* **1978**, *31*, 1211; Chidester, C. G.; et al. *J. Am. Chem. Soc.* **1981**, *103*, 7629), and therefore has been the subject of extensive investigation. Studies have shown that CC-1065 and the duocarmycins tolerate and benefit from structural modifications to the alkylation subunit and that the resulting agents retain their ability to participate in the characteristic sequence selective DNA alkylation reaction (For mechanistic aspects see: Boger, D. L.; Johnson, D. S. *Angew. Chem., Int. Ed. Engl.* **1996**, *35*, 1439; For synthetic aspects see: Boger, D. L.; et al. *Chem. Rev.* **1997**, *97*, 787). Such structural modifications and the definition of their effects have served to advance the understanding of the origin of sequence selectivity (For mechanistic aspects see: Boger, D. L.; Johnson, D. S. *Angew. Chem., Int. Ed. Engl.* **1996**, *35*, 1439; Sun, D.; et al. *Biochemistry* **1993**, *32*, 4487 and references cited therein) and catalysis (Boger, D. L.; Garbaccio, R. M. *Acc. Chem. Res.* **1999**, *32*, 1043; Boger, D. L.; Garbaccio, R. M. *Bioorg. Med. Chem.* **1997**, *5*, 263; Boger, D. L.; et al. *J. Am. Chem. Soc.* **1997**, *119*, 4977; Boger, D. L.; et al. *J. Am. Chem. Soc.* **1997**, *119*, 4987; Warpehoski, M. A.; Hurley, L. H. *Chem. Res. Toxicol.* **1988**, *1*, 315) of the DNA alkylation reaction by **1-3.**

The substitution of the fused pyrrole C ring of CPI, the alkylating subunit of CC-1065 (**3**), with the six-membered benzene ring in CBI was shown to increase relative stability (4×) and biological potency (4×) without affecting DNA alkylation selectivity (Boger, D. L.; et al. *J. Org. Chem.*, **1990**, *55*, 5823; Boger, D. L.; et al. *J. Am. Chem. Soc.* **1989**, *111*, 6461). The preparation of methyl 1,2,9,9a-tetrahydrocyclopropa[*c*]pyrido[3,2-e]indol-4-one-7-carboxylate (CPyI) is disclosed herein. CPyI contains a similar net one carbon expansion of the C ring pyrrole found in the DSA alkylating subunit but with incorporation of a pyridine (Figure 2).

Although there are several well established methods available for selective activation of DNA binding agents including reductive activation (mitomycins),

oxidative activation (aflatoxin), disulfide or trisulfide cleavage (calicheamicin), photochemical activation (psoralen), and oxidant activation of metal complexes (bleomycin), examples of tunable metal cation Lewis acid activation of a DNA alkylating agent are unknown.

Comparative trace metal analysis of cancerous and noncancerous human tissue have revealed significant distinctions (Mulay, I. L.; et al. *J. Natl. Cancer Inst.* **1971**, *47*, 1). Although no generalizations were possible across all tumor types, within a given tumor type these were significant and potentially exploitable differences. For example, Zn was found in breast carcinoma at levels 700% higher than normal breast cells of the same type white lung carcinoma exhibited a revised and even larger 10-fold difference. Thus, chemotherapeutic agents subject to Zn activation can exhibit an enhanced breast carcinoma attributable to this difference in Zn levels (Mulay, I. L.; et al. *J. Natl. Cancer Inst.* **1971**, *47*, 1).

What was needed was a class of DNA alkylating agents employable as cytotoxic agents capable of tunable metal cation Lewis acid activation with Zn and other metals.

Summary:

A new means of *in situ* activation for a class of DNA alkylating agents is disclosed herein. Methyl 1,2,9,9a-tetrahydrocyclopropa[*c*]pyrido[3,2-*e*]indol -4-one-7-carboxylate (CPyl, **17**) contains a unique 8-ketoquinoline structure which provides a tunable means to effect activation *via* selective metal cation complexation (Figure 2). This activation promotes a DNA minor groove adenine N3 alkylation in a manner analogous to that of CC-1065 and the duocarmycins, upon which CPyl was based.

N^2- derivatives of methyl 1,2,9,9a-tetrahydrocyclopropa[*c*]pyrido[3,2-*e*]indol-4-one-7-carboxylate (CPyl) are synthesized and characterized. The unique 8-ketoquinoline structure of CPyl is disclosed to provide a tunable means to affect activation *via* selective metal cation complexation. The synthetic

approach was based on a modified Skraup quinoline synthesis followed by a 5-*exo-trig* aryl radical cyclization onto an unactivated alkene with subsequent TEMPO trap or *5-exo-trig* aryl radical cyclization onto a vinyl chloride for synthesis of the immediate precursor. Closure of the activated cyclopropane, accomplished by an Ar-3' spirocyclization, provided the CPyl nucleus in 10 steps and excellent overall conversion (29%). The evaluation of the CPyl-based agents revealed an intrinsic stability comparable to that of CC-1065 and duocarmycin A, but that it is more reactive than duocarmycin SA and the CBI-based agents (**3–4**). A pH rate profile of the addition of nucleophiles to CPyl demonstrated that an acid-catalyzed reaction is observed below pH 4 and that an un-catalyzed reaction predominates above pH 4. The expected predictable activation of CPyl by metal cations toward nucleophilic addition was found to directly correspond to established stabilities of the metal complexes with the addition product ($Cu^{2+} > Ni^{2+} > Zn^{2+} > Mn^{2+} > Mg^{2+}$), and provides the opportunity to selectively activate the agents upon addition of the appropriate Lewis acid. This tunable metal cation activation of CPyl constitutes the first example of a new approach to *in situ* activation of a DNA binding agent complementary to the well-recognized methods of reductive, oxidative, or photochemical activation. This activation promotes a DNA minor groove adenine N3 alkylation in a manner analogous to that of CC-1065 and the duocarmycins upon which CPyl is based, and represents a new means of *in situ* activation of a novel class of DNA alkylating agents. For the simple alkylation subunit, *N*-BOC-CPyl, an increase in alkylation efficiency of 1000 x was observed in the presence of Zn^{2+} without altering the inherent DNA alkylation selectivity and this efficiency is within 10-fold of the natural products CC-1065 and duocarmycin SA themselves. Resolution and synthesis of a full set of natural product analogues and subsequent evaluation of their DNA alkylation properties revealed that the CPyl analogues retain identical DNA alkylation sequence selectivity and near identical DNA alkylation efficiencies compared to the natural products. Consistent with past studies and even with the deep-seated structural change in the alkylation subunit, the agents were found to exhibit potent cytotoxic activity that directly correlates with their inherent reactivity.

One aspect of the invention is directed to a DNA alkylating agent represented by the following structure:

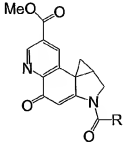

wherein **R** is a DNA minor groove binder. In a preferred embodiment, the DNA alkylating agent is represented by the following structure:

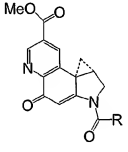

and **R**, the DNA minor groove binder, is represented by one of the following structures:

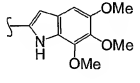

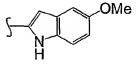

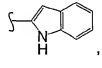

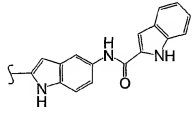

, and

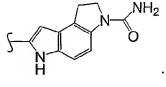

Preferred examples include DNA alkylating agents represented by the following structures:

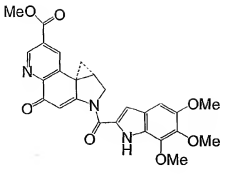

,

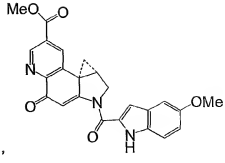

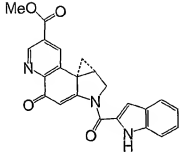

,

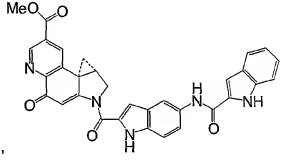

,

and

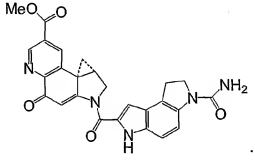

.

Another embodiment of this aspect of the invention is directed to a DNA alkylating agent represented by the following structure:

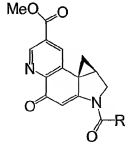

.

In the above structure, **R** represents a DNA minor groove binder, as indicated above.

Another aspect of the invention is directed to a DNA alkylating agent represented by the following structure:

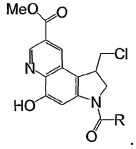

In the above structure, **R** represents a DNA minor groove binder, as indicated above. Preferred embodiments of this aspect of the invention include DNA alkylating agents represented by the following structures :

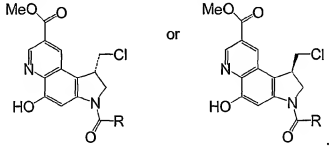

In the above structures, **R** is a DNA minor groove binder represented by any of the following structures:

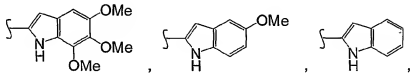

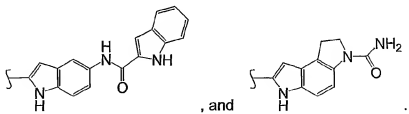

Preferred examples of this aspect of the invention include DNA alkylating agent represented by the following structures:

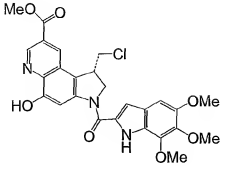

,

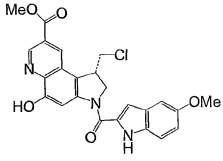

,

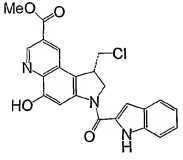

,

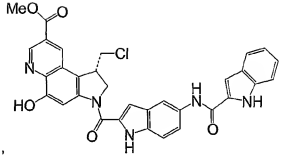

,

and

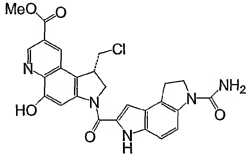

.

Another aspect of the invention is directed to a process for catalyzing a solvolysis of a cyclopropyl ring of an N^2- derivative of methyl 1,2,9,9a-tetrahydrocyclopropa[*c*]pyrido[3,2-*e*]indol-4-one-7-carboxylate. The process employs the step of contacting the N^2- derivative of methyl 1,2,9,9a-tetrahydrocyclopropa[*c*]pyrido[3,2-*e*]indol-4-one-7-carboxylate under aqueous conditions having a pH greater than 4 with a catalytic concentration of a metal ion sufficient to catalyze the solvolysis of the cyclopropyl ring of the N^2- derivative of methyl 1,2,9,9a-tetrahydrocyclopropa[*c*]pyrido[3,2-*e*]indol-4-one-7-carboxylate. The metal ion is selected from Cu^{2+}, Ni^{2+}, Zn^{2+}, Cr^{2+}, Fe^{2+}, Mn^{2+}, and Mg^{2+}. A preferred metal ion is Zn^{2+}.

Another aspect of the invention is directed to a process for catalyzing the production of a DNA alkylation product. The process employs the step of contacting DNA with an N^2- derivative of methyl 1,2,9,9a-tetrahydrocyclopropa[*c*]pyrido[3,2-*e*]indol-4-one-7-carboxylate under aqueous conditions having a pH greater than 4 in the presence of a catalytic concentration of metal ion sufficient to catalyze the alkylation of the DNA by the N^2- derivative of methyl 1,2,9,9a-tetrahydrocyclopropa[*c*]pyrido[3,2-*e*]indol-4-one-7-carboxylate for producing the DNA alkylation product. The metal ion is selected from Cu^{2+}, Ni^{2+}, Zn^{2+}, Cr^{2+}, Fe^{2+}, Cr^{3+}, Fe^{3+}, Mn^{2+}, and Mg^{2+}. A preferred metal ion is Zn^{2+}.

Another aspect of the invention is a DNA alkylation product produced according to the above method.

Another aspect of the invention is directed to a process for catalyzing cell death by DNA alkylation. The process employs the step of contacting a cell, under aqueous conditions having a pH greater than 4, with a concentration of an N^2- derivative of methyl 1,2,9,9a-tetrahydrocyclopropa[*c*]pyrido[3,2-*e*]indol-4-one-7-carboxylate sufficient, in the presence of a catalytic concentration of metal ion, to catalyze cell death by DNA alkylation. The metal ion is selected from Cu^{2+}, Ni^{2+}, Zn^{2+}, Cr^{2+}, Fe^{2+}, Cr^{3+}, Fe^{3+}, Mn^{2+}, and Mg^{2+}. A preferred metal ion is Zn^{2+}.

Brief Description of Figures:

Figure 1 illustrates the structures of naturally occurring DNA alkylating agents, viz.: (+)-duocarmycin SA (**1**) , (+)-duocarmycin A (**2**), and of (+)-CC-1065 (**3**) .

Figure 2 illustrates the structural relationships between CPyl and other DNA alkylating agents, viz.: CPI, CBI, CCBI, MCBI, and DSA. The mechanism of metal chelation and catalysis of solvolysis of the cyclopropyl ring of CPyl is also illustrated.

Figure 3 illustrates the kinetics of solvolysis by UV spectra of *N*-BOC-CPyl (**16**, top) and CPyl (**17**, bottom) in 50% CH_3OH–aqueous buffer (pH 2, 4:1:20 (v:v:v) 1.0 M citric acid, 0.2 M NaH_2PO_4, and H_2O, respectively). The spectra were recorded at regular intervals, and only a few are shown for clarity. Top: (hours) 0, 1, 2, 3, 4, 5, 7, 9, 12, 16, 41. Bottom: (hours) 0, 5, 10, 20, 26, 35, 47, 66, 93, 144, 283.

Figure 4 illustrates a comparison of the rates of solvolysis for *N*-BOC-CPyl with that of *N*-BOC-CPI, *N*-BOC-DA, *N*-BOC-DSA, *N*-BOC-CBI, *N*-BOC-MCBI, *N*-BOC-CCBI, and *N*-BOC-Cl.

Figure 5 illustrates a plot of the log k_{obs} for solvolysis of *N*-BOC-CPyl as a function of pH.

Figure 6 illustrates thermally induced strand cleavage of w794 DNA (SV40 DNA segment, 144 bp, nucleotide nos. 138–5238); DNA–agent incubation for 24 or 48 h, as indicated, at 37 °C, removal of unbound agent and 30 min of thermolysis (100 °C), followed by denaturing 8% PAGE and autoradiography; lanes 1–2, (+)-*N*-BOC-DSA (1 x 10^{-1} and 1 x 10^{-2}); lanes 3–4, (–)-*N*-BOC-DSA (1 x 10^{-1} and 1 x 10^{-2}); lane 5, control DNA; lanes 6–9, Sanger G, C, A and T sequencing reactions; lanes 10–11, (+)-*N*-BOC-CPyl (1 x 10^{-2} and 1 x 10^{-3}); lanes 12–13, (–)-*N*-BOC-CPyl (1 x 10^{-2} and 1 x 10^{-3}); lanes 14–15, (+)-*N*-BOC-CPyl (1 x 10^{-2} and 1 x 10^{-3}); lanes 16–17, (–)-*N*-BOC-CPyl (1 x 10^{-2} and 1 x 10^{-3})

Figure 7 illustrates thermally induced strand cleavage of w794 DNA (SV40 DNA segment, 144 bp, nucleotide nos. 138–5238); DNA–agent incubation for 24 h at 25 °C, removal of unbound agent and 30 min of thermolysis (100 °C), followed by denaturing 8% PAGE and autoradiography; lane 1, control DNA; lanes 2–3, (+)-duocarmycin SA (**1**, 1 x 10^{-5} and 1 x 10^{-6}); lanes 4–6, (+)-CPyl-TMI (**25**, 1 x 10^{-5} to 1 x 10^{-7}); lanes 7–10, Sanger G, C, A and T sequencing reactions; lanes 11–12, (+)-CC-1065 (**3**, 1 x 10^{-5} and 1 x 10^{-6}); lanes 13–15, (+)-CPyl-indole$_2$ (**31**, 1 x 10^{-5} to 1 x 10^{-7}); lanes 16–18, (+)-CPyl-CDPI$_1$ (**33**, 1 x 10^{-5} to 1 x 10^{-7}).

Figure 8 illustrates thermally induced strand cleavage of w794 DNA (SV40 DNA segment, 144 bp, nucleotide nos. 138–5238); DNA–agent incubation for 72 h at 25 °C, removal of unbound agent and 30 min of thermolysis (100 °C), followed by denaturing 8% PAGE and autoradiography; lane 1, control DNA; lanes 2–3, (–)-duocarmycin SA (**1**, 1 x 10^{-5} and 1 x 10^{-6}); lanes 4–5, (–)-CPyI-TMI (**25**, 1 x 10^{-5} and 1 x 10^{-6}); lanes 6–9, Sanger G, C, A and T sequencing reactions; lane 10, (+)-CC-1065 (**3**, 1 x 10^{-6}); lanes 11–12, (–)-CPyI-indole$_2$ (**31**, 1 x 10^{-5} and 1 x 10^{-6}); lanes 13–14, (–)-CPyI-CDPI, (**33**, 1 x 10^{-5} and 1 x 10^{-6}).

Figure 9 illustrates the relative toxicities of various N^2- derivatives of CPyI as compared to CPI, CBI, CCBI, MCBI, and DSA as a function of the particular DNA minor groove binder employed as the N^2- derivative, e.g., BOC, TMI, and CDPI$_1$.

Figure 10 illustrates the aqueous solvolysis of *N*-BOC-CPyI and CPyI (pH 2, phosphate buffer).

Figure 11 illustrates the activation of CPyI by metal cations toward nucleophilic addition and the relative reaction rates of such metal cations, viz., $Cu^{2+} > Ni^{2+} > Zn^{2+} > Cr^{3+} > Fe^{3+} > Mn^{2+} > Mg^{2+}$.

Figure 12 illustrates the enhanced efficiency of the DNA alkylation reaction of CPyI with w794 DNA as a function of the addition of various metal cations, viz.: Cu^{2+} (100x), Ni^{2+} (100-1000x), and Zn^{2+} (1000x).

Figure 13 illustrates a synthetic scheme for CPyI.

Figure 14 illustrates a synthetic scheme for advanced intermediate **14**.

Figure 15 illustrates a synthetic scheme for the synthesis of N^2-derivatives of CPyI using various DNA minor groove binders.

Figure 16 illustrates an acid-catalyzed nucleophilic addition of CH_3OH to **16**.

Figure 17 illustrates a comparison of the treatment of *N*-BOC-CPyl (**16**) with $Zn(OTf)_2$ in CH_3OH to provide a single product **41** with the inability of *N*-BOC-CBI (**37**) to similarly exhibit this metal-catalyzed reactivity in the presence of $Zn(OTf)_2$.

Figure 18 illustrates solvolysis rates of CPyl and *N*-BOC-CPyl with phosphate buffer.

Figure 19 illustrates solvolysis rates of *N*-BOC-CPyl with universal buffer.

Figure 20 illustrates the *in vitro* cytotoxicity of various N^2- derivatives of CPyl.

Figure 21 illustrates thermally induced strand cleavage of w794 DNA (SV40 DNA segment, 144 bp, nucleotide nos. 138–5238); DNA–agent incubation for 24 h at 25 °C, removal of unbound agent and 30 min of thermolysis (100 °C), followed by denaturing 8% PAGE and autoradiography; lanes 1, control DNA with $Zn(acac)_2$ (1×10^0 M); lanes 2-5, (+)-*N*-BOC-CPyl (**16**, 1×10^{-2} to 1×10^{-5} M); lanes 6-7, (+)-duocarmycin SA (1×10^{-5} and 1×10^{-6} M); lanes 8–11, Sanger G, C, A and T sequencing reactions; lane 12, (+)-*N*-BOC-CPyl (**16**, 1×10^{-3} M) with $Zn(acac)_2$ (1 equiv); lanes 13-15, (+)-*N*-BOC-CPyl (**16**, 1×10^{-4} M) with $Zn(acac)_2$ (1, 10, and 100 equiv); lanes 16-17, (+)-*N*-BOC-CPyl (**16**, 1×10^{-5} M) with $Zn(acac)_2$ (1 and 1000 equiv).

Detailed Description:

A short and efficient 10 step (29% overall) synthesis of CPyl featuring a modified Skraup quinoline synthesis followed by a *5-exo-trig* aryl radical cyclization onto a vinyl chloride is detailed and constitutes a net one carbon expansion of the C ring pyrrole found in the duocarmycin SA alkylation subunit. CPyl was found to be 3-4x less stable than CBI and duocarmycin SA but possesses a superior stability to CC-1065 and duocarmycin A. Nucleophilic addition occurred at the least substituted cyclopropane carbon with a regioselectivity (>20:1) comparable to that of CBI but which exceeds that of the natural products themselves (6-1.5:1). A pH rate profile of the addition of nucleophiles to CPyl demonstrated that it is an acid-catalyzed reaction below pH 4, but an uncatalyzed reaction above pH 4 consistent with the observation that the DNA alkylation reaction at physiological pH is not acid-catalyzed (Boger, D. L.; Garbaccio, R. M. *Acc. Chem. Res.* **1999**, *32*, 1043; Boger, D. L.; Garbaccio, R. M. *Bioorg. Med. Chem.* **1997**, *5*, 263; Boger, D. L.; et al. *J. Am. Chem. Soc.* **1997**, *119*, 4977; Boger, D. L.; et al. *J. Am. Chem. Soc.* **1997**, *119*, 4987; Boger, D. L.; Garbaccio, R. M. *J. Org. Chem.* **1999**, *64*, 5666; Boger, D. L.; Turnbull, P. *J. Org. Chem.* **1998**, *63*, 8004; Boger, D. L.; Turnbull, P. *J. Org. Chem.* **1997**, *62*, 5849; Boger, D. L.; et al. *Bioorg. Med. Chem. Lett.* **1997**, *7*, 233). The tunable activation of CPyl by metal cations toward nucleophilic addition, which directly follows established stabilities of the resulting metal complexes with the addition product ($Cu^{2+} > Ni^{2+} > Zn^{2+} > Mn^{2+} > Mg^{2+}$), provides the opportunity to selectively and predictably initiate reactions of the agent simply by addition of the appropriate Lewis acid. This novel activation arises from chelation to the CPyl 8-ketoquinoline core, a unique structural feature that is not found in the natural products or alkylation subunit analogues disclosed to date. Resolution and incorporation of CPyl into a full set of duocarmycin and CC-1065 analogues allowed for examination of their cytotoxic and DNA alkylation properties. The CPyl analogues were potent cytotoxic agents exhibiting picomolar IC_{50}'s which correlated with their relative stability. In addition to smoothly following this correlation, the analogues displayed a smooth trend of increasing cytotoxic potency with the increasing length in the DNA binding subunit. Analogous to the natural products, the (*S*)-enantiomers possessing the

absolute configuration of **1-3**, proved to be more potent (3-30x) than the unnatural (*R*)-enantiomers. DNA alkylation studies revealed that the CPyl analogues exhibited an identical DNA alkylation sequence selectivity and near identical DNA alkylation efficiencies compared to the natural products. Thus, this set of analogues, which contain a unique structural modification in the alkylation subunit, retain full DNA alkylation and cytotoxic properties of the natural products, while possessing a novel capability for predictable and tunable activation by chelation of Lewis acids. Although this Lewis acid activation is of limited use for agents which already display effective DNA alkylation properties, its use is especially effective when applied to CPyl members which are poor at alkylating DNA. This includes *N*-BOC-CPyl (**16**) for which the alkylation efficiency is increased 10^5× and reversed analogs of CPyl in which the DNA binding subunits are attached through the C-terminus methyl ester rather than N-terminus secondary amine.

Synthesis of *N*-BOC-CPyl. The CPyl synthesis was based on a modified Skraup quinoline synthesis to provide the core structure, followed by the TEMPO trap of an aryl radical-alkene 5-*exo*-*trig* cyclization for introduction of the A-ring, and final Ar-3' spirocyclization (Figure 13). Thus, 2-bromoacrolein was treated with **4** in the presence of bromine (1.0 equiv, AcOH, 100 °C, 1 h, 92%) to provide **5** (Baker, R. H.; et al. *J. Am. Chem. Soc.* **1950**, *72*, 393; Tinsley, S. W. *J. Am. Chem. Soc.* **1955**, *77*, 4175). Protection of phenol **5** (1.2 equiv of BnBr, 1.1 equiv of NaH, DMF, 4 to 25 °C, 24 h, 85%) was followed by nitro reduction with $SnCl_2$ (5.0 equiv, EtOAc, 0.5 h, 70 °C), and amine protection (4.0 equiv of $(BOC)_2O$, 2 equiv of Et_3N, dioxane, 70 °C, 1 h, 74% for two steps). The resultant 3-bromoquinoline **7** was subjected to Pd(0)-catalyzed carboxybutylation (Schoenberg, A.; et al. *J. Org. Chem.* **1974**, *39*, 3318; Heck, R. F. *Palladium Reagents in Organic Synthesis,* Academic Press: London, Orlando (Fla), 1985) (0.1 equiv of $(PPh_3)_4Pd$, CO (g), 1.2 equiv of *n*-Bu_3N, *n*-BuOH, 100 °C, 12 h, 78%) and treatment with LiOMe (1.1 equiv, MeOH, 25 °C, 1.5 h, 91%) to afford **9**. As detailed by Heck (Schoenberg, A.; et al. *J. Org. Chem.* **1974**, *39*, 3318; Heck, R. F. *Palladium Reagents in Organic Synthesis,* Academic Press: London, Orlando (Fla), 1985), the use of MeOH as a reaction solvent for direct Pd-mediated

carboxymethylation of **7** is limited by the achievable reaction temperatures (65 °C with MeOH versus 115 °C with *n*-BuOH) and thus requires extended reaction times (≥ 3 d) and generally proceeds in lower yields (≤ 45%). Following selective, acid-catalyzed C5 iodination (Boger, D. L.; McKie, J. A. *J. Org. Chem.* **1995**, *60*, 1271) of **9** with *N*-iodosuccinimide (1.2 equiv, cat. TsOH, THF-CH_3OH, 0 to 25 °C, 1 d, 88%), *N*-alkylation of the sodium salt of **10** (1.1 equiv of NaH, DMF, 4 °C, 30 min) with allyl bromide (3 equiv, DMF, 25 °C, 2.5 h, 94%) proceeded smoothly.

In contrast to related substrates (For synthetic aspects see: Boger, D. L.; et al. *Chem. Rev.* **1997**, *97*, 787; Boger, D. L.; McKie, J. A. *J. Org. Chem.* **1995**, *60*, 1271), cyclization of **11** under previously described conditions (6.0 equiv of Bu_3SnH, 6.0 equiv of TEMPO, 70 °C, benzene, 3.5 h) did not proceed in high yield (41-54%). Although tin hydride-mediated reduction has been observed with similar compounds (Ueno, Y.; et al. *Tetrahedron Lett.* **1982**, *23*, 2575; Shankaran, K.; et al. *Tetrahedron Lett.* **1985**, *26*, 6001), it had not been observed in other CC-1065/duocarmycin systems. Consequently, it was surprising to isolate significant amounts (≥ 30%) of the halogen-reduced product. Characterization of this byproduct (Methyl 8-(benzyloxy)-6-[(*N*-(*tert*-butyloxycarbonyl)- *N*-(2-propenyl))amino]quinoline-3-carboxylate: FABHRMS (NBA/CsI) *m/z* 581.1065 (M + Cs^+, $C_{26}H_{28}N_2O_5$ requires 581.1053)) was confirmed by direct comparison with an authentic sample prepared by allylation of **9** (3 equiv of allyl bromide, 1.1 equiv of NaH, DMF, 4 to 25 °C, 89%). The radical cyclization was improved utilizing *tris*(trimethylsilyl)silane, $((CH_3Si)_3SiH$, 5 equiv, 8.0 equiv of TEMPO, toluene, 80 °C, 16 h, 85%), which has a stronger metal-hydride bond than Bu_3SnH (79 vs. 74 kcal/mol) (Giese, B.; Kopping, B. *Tetrahedron Lett.* **1989**, *30*, 681; Kanabus-Kaminska, J. M.; et al. *J. Am. Chem. Soc.* **1987**, *109*, 5267) and therefore a slower rate of aryl radical reduction permitting clean intramolecular 5-*exo*-*trig* cyclization. The TEMPO trapped product **12** was reduced with activated Zn (Boger, D. L.; McKie, J. A. *J. Org. Chem.* **1995**, *60*, 1271; Newman, M. S.; Evans, F. J., Jr. *J. Am. Chem. Soc.* **1955**, *77*, 946) (50 equiv, 3:1 HOAc-THF, 60 °C, 11 h, 60%) and the resulting alcohol **13** converted to the primary chloride (Hooz, J.; Gilani, S. S. H. *Can. J. Chem.* **1968**, *46*, 86) (3.0 equiv of Ph_3P, 9.0 equiv of CCl_4, CH_2Cl_2, 25 °C, 3 h, 73%). Two-phase transfer

catalytic hydrogenolysis (Ram, S.; Ehrenkaufer, R. E. *Synthesis* **1988**, 91; Bieg, T.; Szeja, W. *Synthesis* **1985**, 76) of the benzyl ether **14** (10% Pd-C, 10 equiv 25% aqueous HCO_2NH_4, 25 °C, 3 h, 99%) and subsequent spirocyclization (Baird, R.; Winstein, S. *J. Am. Chem. Soc.* **1963**, *85*, 567; Baird, R.; Winstein, S. *J. Am. Chem. Soc.* **1962**, *84*, 788; Winstein, S.; Baird, R. *J. Am. Chem. Soc.* **1957**, *79*, 756) by treatment of **15** with DBU (3 equiv, CH_3CN, 25 °C, 3 h, 99%) provided *N*-BOC-CPyI (**16**). Acid-catalyzed deprotection of **16** (3 M HCl-EtOAc, 25 °C, 30 min), which is accompanied by the addition of chloride to the cyclopropane, followed by treatment of the crude hydrochloride salt with K_2CO_3 (10 equiv, acetone, 25 °C, 24 h, 96%) cleanly provided CPyI (**17**).

In an improved preparation of the advanced (chloromethyl)indoline precursor, adoption of a direct free radical cyclization (Patel, V. F.; et al. *J. Org. Chem.* **1997**, *62*, 8868; Boger, D. L.; et al. *Tetrahedron Lett.* **1998**, *39*, 2227) of a substrate bearing a vinyl chloride acceptor alkene provided **14** in good conversion (Figure 14). Thus, alkylation of the sodium salt of **10** (1.1 equiv of NaH, DMF, 4 °C, 30 min) with *E*-1,3-dichloropropene (3 equiv, 25 °C, 12 h, 94%) was followed by free radical cyclization of the vinyl chloride (1.5 equiv of Bu_3SnH, cat. AIBN, benzene, 70 °C, 6.5 h, 87%) to provide **14**. The incorporation of this improvement provided *N*-BOC-CPyI (**16**) in 10 steps and superb overall conversion (29%).

Resolution. In order to assess the properties of both enantiomers of the CPyI based agents, a direct chromatographic resolution on a ChiralCel-OD semi-preparative HPLC column (2 × 25 cm, 50% *i*-PrOH-hexanes eluant, 7 mL/min, α = 1.43) provided both enantiomers of **16** (>99% ee). *N*-BOC-CPyI proved to be the only late-stage intermediate that could be effectively resolved on a ChiralCel-OD column, and similar efforts to separate **13-15** were not successful. The slower eluting (+)-enantiomer of **16** (t_R = 38 min) was assigned the natural (3*S*)-configuration and agents derived from this (+)-enantiomer exhibited the more potent biological activity, the more effective DNA alkylation properties, and a DNA alkylation selectivity identical with the natural products. The faster eluting (-)-enantiomer of **16** (t_R = 27 min) was assigned the unnatural (3*R*)-configuration

and agents derived from this (-)-enantiomer exhibited the corresponding less potent biological activity, the less effective DNA alkylation properties, and a DNA alkylation selectivity identical with the unnatural enantiomers of the natural products.

Synthesis of Duocarmycin and CC-1065 Analogues. The CPyl alkylation subunit was incorporated into duocarmycin and CC-1065 analogues as detailed in Figure 15. Deprotection and concurrent ring opening of **16** (3 M HCl-EtOAc) followed by immediate coupling (4 equiv of EDCI, DMF, 25 °C) of the resulting amine hydrochloride salt with 5,6,7-trimethoxyindole-2-carboxylic acid (Boger, D. L.; et al. *J. Am. Chem. Soc.* **1990**, *112*, 8961) (TMI, **19**, 10 h, 52%), 5-methoxyindole-2-carboxylic acid (**20**, 10 h, 59%), indole-2-carboxylic acid (**21**, 10 h, 71%), $indole_2$ (Boger, D. L.; et al. *Bioorg. Med. Chem.* **1995**, *3*, 1429) (**22**, 16 h, 64%), and $CDPI_1$ (Boger, D. L.; et al. *J. Org. Chem.* **1987**, *52*, 1521; Boger, D. L.; Coleman, R. S. *J. Org. Chem.* **1984**, *49*, 2240) (**23**, 16 h, 41%) provided **24**, **26**, **28**, **30**, and **32**, respectively. DBU (3 equiv, 3 h, 25 °C) promoted spirocyclization of **24** (DMF, 86%), **26** (CH_3CN, 90%), **28** (CH_3CN, 93%), **30** (DMF, 97%), and **32** (DMF, 67%) provided **25**, **27**, **29**, **31**, and **33**, respectively.

Solvolysis: Reactivity and Regioselectivity. Two fundamental characteristics of the alkylation subunits have proven important in past studies (For mechanistic aspects see: Boger, D. L.; Johnson, D. S. *Angew. Chem., Int. Ed. Engl.* **1996**, *35*, 1439). The first is the stereo-electronically-controlled acid-catalyzed ring opening of the activated cyclopropane which dictates preferential addition of a nucleophile to the least substituted cyclopropane carbon. The second is the relative reactivity of the agents as established by their rate of acid-catalyzed solvolysis which has been found to accurately reflect a direct relationship between intrinsic stability and *in vitro* cytotoxicity (For mechanistic aspects see: Boger, D. L.; Johnson, D. S. *Angew. Chem., Int. Ed. Engl.* **1996**, *35*, 1439).

Solvolysis was conducted in 50% CH_3OH-buffer mixtures (pH 3 buffer = 4:1:20 (v:v:v) 0.1 M citric acid: 0.2 M Na_2HPO_4: H_2O; pH 2 buffer = 4:1:20 (v:v:v) 1.0 M citric acid: 0.2 M Na_2HPO_4: H_2O) and followed spectrophotometrically by UV with the disappearance of the long-wavelength absorption of the CPyl

chromophore and with the appearance of a short-wavelength absorption attributable to the solvolysis product (Figures 3 and 18). *N*-BOC-CPyl (**16**) proved to be reasonably stable to solvolysis even at pH 2.0 ($k = 3.72 \times 10^{-8}$ s^{-1}, $t_{1/2}$ = 5.2 h) and pH 3.0 ($k = 3.81 \times 10^{-6}$ s^{-1}, $t_{1/2}$ = 50.5 h) as compared to *N*-BOC-CPI (**34**, pH 3, $t_{1/2}$ = 37 h) and *N*-BOC-DA (**35**, pH 3, $t_{1/2}$ = 11 h) (Figure 4). However, **16** was less stable than *N*-BOC-DSA (**36**, pH 3, $t_{1/2}$ = 177 h) and *N*-BOC-CBI (**37**, pH 3, $t_{1/2}$ = 133 h). The rate of solvolysis was found to be independent of the phosphate buffer countercation (Na^+, NH_4^+ or K^+) within experimental error.

The acid-catalyzed nucleophilic addition of CH_3OH to **16** was conducted on a preparative scale to establish the regioselectivity of addition and was confirmed by synthesis of the expected product **41** derived from nucleophilic addition to the least substituted cyclopropane carbon. Treatment of *N*-BOC-CPyl (**16**) with catalytic CF_3SO_3H (0.3 equiv, CH_3OH, 25 °C, 20 h, 91%) resulted in the clean addition to provide a single product **41** (Figure 16). Similarly, treatment of **16** with HCl-EtOAc (2 equiv, THF, -78 °C, 2 min, 96%) provided **15** as a single product. Clean cleavage of the C8b-C9 bond with S_N2 addition of CH_3OH or HCl to the least substituted C9 cyclopropane carbon was observed, and no cleavage of the C8b-C9a bond with ring expansion was detected (>20:1). This is in sharp contrast to the natural products where substantial amounts of the alternative ring expansion addition products have been observed (6-1.5:1) (Warpehoski, M. A.; Harper, D. E. *J. Am. Chem. Soc.* **1984**, *116*, 7573; Warpehoski, M. A.; Harper, D. E. *J. Am. Chem. Soc.* **1995**, *117*, 2951; Boger, D. L.; et al. *Bioorg. Med. Chem. Lett.* **1996**, *6*, 1955; Boger, D. L.; et al. *J. Am. Chem. Soc.* **1997**, *119*, 311; Boger, D. L.; et al. *J. Org. Chem.* **1996**, *61*, 1710; Boger, D. L.; et al. *J. Org. Chem.* **1996**, *61*, 4894). Nonetheless, the observations are consistent with prior studies with *N*-BOC-CBI (**37**), *N*-BOC-MCBI (**38**), and *N*-BOC-CCBI (**39**) where no (>20:1) ring expansion solvolysis product was detected (Figure 4) (Boger, D. L.; et al. *J. Am. Chem. Soc.* **1990**, *112*, 8961; Boger, D. L.; et al. *J. Org. Chem.* **1996**, *61*, 1710; Boger, D. L.; et al. *J. Org. Chem.* **1996**, *61*, 4894).

Solvolysis pH Dependence. Duocarmycin SA (**1**) is known to be exceptionally stable at neutral conditions and it was interesting to observe that *N*-BOC-CPyl (**16**) possessed measurably solvolytic reactivity in 50% aqueous CH_3OH (pH 7).

A full pH rate profile in 50% CH_3OH-universal buffer (pH 2-12, $B(OH)_3$-citric acid-Na_3PO_4) (Perrin, D. D.; Dempsey, B. *Buffers for pH and Metal Ion Control;* Chapman and Hall: London, 1979; p 156) demonstrated a near first-order rate dependence on acid at pH 2-4 (Figures 5 and 19). Above pH 4, the dependence on acid concentration disappeared indicating a change in mechanism from acid-catalyzed solvolysis to one which is uncatalyzed. A loss of isobestic behavior in the UV trace at pH 11 indicated a second reaction event at this pH, presumably arising from hydrolysis of either the BOC or methyl ester. From a regression analysis best fit plot of the k_{obs} versus pH, rate constants of 3.37×10^{-3} $M^{-1}s^{-1}$ and 8.36×10^{-7} s^{-1} for the acid-catalyzed and uncatalyzed reactions, respectively, were established. This, plus the demonstration that related reactions above pH 4 are not only not specific acid-catalyzed, but also not general acid-catalyzed (Boger, D. L.; Garbaccio, R. M. *J. Org. Chem.* **1999**, *64*, 5666; Boger, D. L.; Turnbull, P. *J. Org. Chem.* **1998**, *63*, 8004; Boger, D. L.; Turnbull, P. *J. Org. Chem.* **1997**, *62*, 5849; Boger, D. L.; et al. *Bioorg. Med. Chem. Lett.* **1997**, *7*, 233), suggest this is simply an uncatalyzed S_N2 nucleophilic addition. The demonstration of an uncatalyzed solvolysis above pH 4 is consistent with the observation that the DNA alkylation reaction at the physiological pH of 7.6 is not acid-catalyzed and that catalysis must come from an alternative source (Boger, D. L.; Garbaccio, R. M. *Acc. Chem. Res.* **1999**, *32*, 1043; Boger, D. L.; Garbaccio, R. M. *Bioorg. Med. Chem.* **1997**, *5*, 263; Boger, D. L.; et al. *J. Am. Chem. Soc.* **1997**, *119*, 4977; Boger, D. L.; et al. *J. Am. Chem. Soc.* **1997**, *119*, 4987; Boger, D. L.; Garbaccio, R. M. *J. Org. Chem.* **1999**, *64*, 5666; Boger, D. L.; Turnbull, P. *J. Org. Chem.* **1998**, *63*, 8004; Boger, D. L.; Turnbull, P. *J. Org. Chem.* **1997**, *62*, 5849; Boger, D. L.; et al. *Bioorg. Med. Chem. Lett.* **1997**, *7*, 233).

Solvolysis: Metal Catalysis. Central to the projected use of the CPyl agents and their potential of metal cation activation was their reactivity in the presence of metal cations (Boger, D. L.; et al. *J. Am. Chem. Soc.* **1993**, *115*, 10733; Yoshida, K.; et al. *Bull. Chem. Soc. Jpn.* **1988**, *61*, 4335; Yoshida, K.; et al. *Chem. Lett.* **1986**, 1059; Pratt, Y. T. *J. Org. Chem.* **1962**, *27*, 3905). Treatment of *N*-BOC-CPyl (**16**) with $Zn(OTf)_2$ (1.1 equiv) in CH_3OH (25 °C, 4 h, 92%) on a

preparative scale resulted in clean addition to provide a single product **41** (Figure 17). In contrast, *N*-BOC-CBI (**37**) did not exhibit this metal-catalyzed reactivity in the presence of $Zn(OTf)_2$ (1.5 equiv, CH_3OH, 27 h, 25 °C, 100% recovery), confirming that the CPyl 8-ketoquinoline structure is key to metal chelation, activation, and Lewis acid-catalyzed reaction.

The rates of metal-catalyzed (Cu^{2+}, Ni^{2+}, Zn^{2+}, Mn^{2+}, Mg^{2+}, Mg^{2+}, Fe^{3+}, Cr^{3+}, and Ti^{4+}) addition to *N*-BOC-CPyl (**16**) in CH_3OH were measured spectrophotometrically by UV with the disappearance of the long-wavelength absorption of the CPyl chromophore and with the appearance of a short-wavelength absorption (Figure 11). Within a series of divalent metals with acetylacetonate (acac) ligands, the relative rates of solvolysis (rate: $Cu^{2+} > Ni^{2+} > Zn^{2+} > Mn^{2+} > Mg^{2+}$) corresponded directly with established stability constants of the metal complexes with 8-hydroxyquinoline (stability: $Cu^{2+} > Ni^{2+} > Zn^{2+} > Mn^{2+} > Mg^{2+}$) (Phillips, J. P. *Chem. Rev.* **1956**, *56*, 271; Irving, H.; Williams, R. J. P. *J. Chem. Soc.* **1953**, 3192). Higher valence metals including Fe^{3+}, Cr^{3+}, and Ti^{4+} also demonstrated an analogous activation of CPyl for nucleophilic addition. Notably, no apparent catalysis was observed for $Mg(acac)_2$ over and beyond the background rate indicating that this endogenous metal cation, like Na^+, does not activate CPyl effectively. Stronger Lewis acids were found to provide at a faster reaction rate ($Zn(OTf)_2$: $t_{1/2}$ = 0.8 h versus $Zn(acac)_2$: $t_{1/2}$ = 11.5 h) and incorporation of H_2O in the solvent slowed the reaction ($Zn(OTf)_2$, 50% aqueous CH_3OH, $t_{1/2}$ = 33 h). *N*-BOC-CBI (**37**) demonstrated no detectable reaction in the $Zn(OTf)_2$-CH_3OH system after 7 d, further confirming the role of metal cation catalysis for CPyl. Thus, the well-behaved activation of CPyl predictably tunable by choice of the metal cation provides the opportunities to selectively activate the agents.

DNA Alkylation Selectivity and Efficiency. The DNA alkylation properties of the agents were examined within w794 duplex DNA (Boger, D. L.; et al. *Tetrahedron* **1991**, *47*, 2661) for which comparative results are available for related agents (For mechanistic aspects see: Boger, D. L.; Johnson, D. S. *Angew. Chem., Int. Ed. Engl.* **1996**, *35*, 1439). The alkylation site identification

and the assessment of the relative selectivity among the available sites were obtained by thermally-induced strand cleavage of the singly 5' end-labeled duplex DNA after exposure to the agents. Following treatment of the end-labeled duplex DNA with a range of agent concentrations and temperatures in the dark, the unbound agent was removed by EtOH precipitation of the DNA. Redissolution of the DNA in aqueous buffer, thermolysis (100 °C, 30 min) to induce strand cleavage at the sites of DNA alkylation, denaturing high-resolution polyacrylamide gel electrophoresis (PAGE) adjacent to Sanger dideoxynucleotide sequencing standards, and autoradiography led to identification of the DNA cleavage and alkylation sites. The full details of this procedure have been disclosed elsewhere (Boger, D. L.; et al. *Tetrahedron* **1991**, *47*, 2661). A representative comparison of the DNA alkylation properties of both enantiomers of *N*-BOC-CPyl (**16**) alongside both enantiomers of *N*-BOC-DSA (**36**) is presented in Figure 6. Both natural enantiomers exhibited approximately the same efficiencies of DNA alkylation detectable at 10^{-3} M (37 °C, 48 h) and prominent at 10^{-2} M. (+)-*N*-BOC-CPyl was slightly less efficient than the unnatural enantiomer, (-)-*N*-BOC-CPyl, at both 24 and 48 h incubations which is also reflected in the relative cytotoxic activities of the two enantiomers. Like the preceding BOC derivatives examined (For mechanistic aspects see: Boger, D. L.; Johnson, D. S. *Angew. Chem., Int. Ed. Engl.* **1996**, *35*, 1439), **16** alkylated DNA much less efficiently than **24-33** (10^4x), providing detectable alkylation at 10^{-2}-10^{-3} M only under vigorous conditions (37 °C, 24-72 h) and much less selectively than **24-33**, exhibiting a two-base pair AT-rich alkylation selectivity (5'-A<u>A</u> > 5'-T<u>A</u>). This unusual behavior of the two enantiomers alkylating the same sites is analogous to past observations (For mechanistic aspects see: Boger, D. L.; Johnson, D. S. *Angew. Chem., Int. Ed. Engl.* **1996**, *35*, 1439). It is a natural consequence of the reversed binding orientation of the two enantiomers and the diastereomeric relationship of the two adducts that result in the two enantiomers covering the exact same binding site surrounding the alkylated adenine. This has been discussed in detail illustrated elsewhere, and *N*-BOC-CPyl (**16**) conforms nicely to these past observations and models (For mechanistic aspects see: Boger, D. L.; Johnson, D. S. *Angew. Chem., Int. Ed. Engl.* **1996**, *35*, 1439).

A representative comparison of the DNA alkylation by (+)-CPyl-TMI (**25**),

(+)-CPyI-indole$_2$ (**31**), and (+)-CPyI-CDPI$_1$ (**33**) alongside that of (+)-duocarmycin SA (**1**) and (+)-CC-1065 (**3**) within w794 DNA is illustrated in Figure 7. (+)-CPyI-TMI and (+)-duocarmycin SA alkylate DNA with identical selectivity and near identical efficiency with the latter agent being slightly more effective. This is nicely illustrated in Figure 7 where the two agents detectably alkylate the same high affinity site of 5'-AATTA at 10^{-6}-10^{-7} M (25 °C, 24 h). This is analogous to the observations made in comparisons of duocarmycin SA and CBI-TMI (Boger, D. L.; Yun, W. *J. Am. Chem. Soc.* **1994**, *116*, 7996). Like the preceding agents, the CPyI-based agents exhibit AT-rich adenine N3 alkylation selectivities that start at the 3' adenine N3 alkylation site with agent binding in the minor groove in the 3' to 5' direction covering 3.5 or 5 base pairs (data not shown).

A representative comparison of the DNA alkylation by (-)-CPyI-TMI (**25**), (-)-CPyI-indole$_2$ (**31**),and (-)-CPyI-CDPI$_1$ (**33**) alongside the unnatural enantiomer of duocarmycin SA (**1**) and the natural enantiomer of CC-1065 (**3**) within w794 DNA is illustrated in Figure 8. The unnatural enantiomer DNA alkylation is considerably slower, and the results shown in Figure 8 were obtained only with their incubation for 72 h (25 °C) versus incubation for 24 h (25 °C, Figure 7) for the natural enantiomers. Despite the longer reaction times, the extent of alkylation by the unnatural enantiomers is lower, requiring higher agent concentrations to detect. The DNA alkylation selectivity and efficiency observed with *ent*-(-)-CPyI-TMI (**25**) and *ent*-(-)-duocarmycin SA (**1**) were indistinguishable with the latter agent being slightly more effective. The alkylation sites for the unnatural enantiomers proved consistent with adenine N3 alkylation with agent binding in the minor groove in the reverse 5' to 3' direction across a 3.5 or 5 base-pair AT-rich site surrounding the alkylation site (data not shown). This is analogous to the natural enantiomer alkylation selectivity except that it extends in the reverse 5' to 3' direction in the minor groove and, because of the diastereomeric nature of the adducts, is offset by one base pair relative to the natural enantiomers.

In **Vitro Cytotoxic Activity.** Past studies with agents in this class have defined a direct correlation between inherent stability and cytotoxic potency (For mechanistic aspects see: Boger, D. L.; Johnson, D. S. *Angew. Chem., Int. Ed.*

Engl. **1996**, *35*, 1439). Consistent with their relative reactivity, the CPyl based agents exhibited cytotoxic activity that closely followed this relationship (Figures 9 and 20) (For mechanistic aspects see: Boger, D. L.; Johnson, D. S. *Angew. Chem., Int. Ed. Engl.* **1996**, *35*, 1439). The results, which also follow trends established in the DNA alkylation studies, demonstrate that the (+)-enantiomer of the analogs possessing the configuration of the natural products, is the more potent enantiomer by 3-30x. The exceptions to this trend are the simple alkylation subunits **16** and **17** themselves which, like others in the series, typically exhibit comparable activities. The seco precursors, which lack the preformed cyclopropane but possess the capabilities of ring closure, were found to possess cytotoxic activity that was indistinguishable from the final ring-closed agents. Consistent with the unique importance of the C5 methoxy group in the binding subunit of the duocarmycins (Boger, D. L.; Garbaccio, R. M. *Acc. Chem. Res.* **1999**, *32*, 1043; Boger, D. L.; Garbaccio, R. M. *Bioorg. Med. Chem.* **1997**, *5*, 263; Boger, D. L.; et al. *J. Am. Chem. Soc.* **1997**, *119*, 4977; Boger, D. L.; et al. *J. Am. Chem. Soc.* **1997**, *119*, 4987), CPyl-TMI (**25**) and **27** were found to be equipotent illustrating that the C6 and C7 methoxy groups of **25** are not contributing to its cytotoxic potency. The indole derivative **29** was found to be less potent (10x) than both **25** and **27**, further demonstrating the importance of the C5 methoxy which we have suggested is derived from extending the rigid length of the agents and contributing to the alkylation catalysis (Boger, D. L.; Garbaccio, R. M. *Acc. Chem. Res.* **1999**, *32*, 1043; Boger, D. L.; Garbaccio, R. M. *Bioorg. Med. Chem.* **1997**, *5*, 263; Boger, D. L.; et al. *J. Am. Chem. Soc.* **1997**, *119*, 4977; Boger, D. L.; et al. *J. Am. Chem. Soc.* **1997**, *119*, 4987). Finally, the longer agents, CPyl-indole$_2$ (**31**) and CPyl-CDPI$_1$ (**33**), displayed the most potent cytotoxic activity reflecting their longer length and greater adduct stability.

Metal Activation of CPyl:

A study of CPyl activation by metal cations toward nucleophilic addition (MeOH, Figure 11) revealed that the relative reaction rates correspond to the established stabilities of the resulting metal complexes (8-hydroxyquinoline, Cu^{2+} > Ni^{2+} > Zn^{2+} > Mn^{2+} > Mg^{2+}) (J. P. Phillips, *Chem. Rev.* **1956**, *56*, 271; and H.

Irving, et al., *J. Chem. Soc.* **1953**, 3192). This provides the opportunity to predict, control, and tune the reactivity over a wide range depending on the application and conditions. Notably, Mg^{2+} provided a rate which was not distinguishable from a background rate of BOC methanolysis, indicating that this prominent endogenous metal cation, like Na^{+}, does not appear to activate CPyl effectively.

Consistent with this behavior, the efficiency of the DNA alkylation reaction of **16** (w794 DNA) (see: D. L. Boger, et al., *Tetrahedron* **1991**, *47*, 2661), which occurs at 10^{-2} M for 1-3 (24 h, 25 °C for 1, 37 °C for 2 and 3), was dramatically increased in the presence of Cu^{2+} (100x), Ni^{2+} (100-1000x), and Zn^{2+} (1000x), the three metals selected for study, Figure 12. This enhancement increased with increasing metal cation concentration for **16**, but not **35** and **36**, and resulted in no change in the DNA alkylation selectivity of **16**, which was identical to **35** and **36**. Typically studies were conducted with 1, 10, 100, 1000 equivalents of the metal cation with the former producing significant effects and the latter two concentrations providing the maximal effects. Under the conditions of the measurements reported herein, the enhancement was especially remarkable with Zn^{2+} (1000x) which promoted DNA alkylation of **16** at 10^{-5} M. This greater behavior of Zn^{2+} relative to Ni^{2+} and Cu^{2+} ($Zn^{2+} > Ni^{2+} > Cu^{2+}$) is attributed not to an alteration in the relative activations from that expected ($Cu^{2+} > Ni^{2+} > Zn^{2+}$), but rather to an enhanced selectivity under the reaction conditions employed. That is, the greater activation by Cu^{2+} and Ni^{2+} leads to more nonproductive solvolysis relative to Zn^{2+}, lowering the apparent efficiencies of DNA alkylation. For any given application, the optimal results are going to depend on the reaction conditions (solvent, buffer, temperature, time) and the optimal catalyst from the range of metal cation catalysts can be established to tune the reactivity. Alkylation at such low concentrations is unprecedented for such simple alkylation subunits and this efficiency is within 10-fold of the natural product (+)-duocarmycin SA (10^{-6} M, 25 °C), Figure 21. Similar enhancements in the rates of DNA alkylation were also observed. Analogous metal cation enhancements in the rates and efficiency of DNA alkylation for the unnatural enantiomer of **16** were also observed (data not shown). However, similar treatments of **35** and **36** (alkylation at 10^{-2} M) or duocarmycin SA and CC-1065 (alkylation at 10^{-6} M) did

not affect their DNA alkylation rates or efficiencies (data not shown) indicating this behavior is unique to CPyI (**16**) and its 8-ketoquinoline core structure.

In addition to representing a new and tunable method of in situ activation of a novel class of DNA alkylating agents, the observations have implications on the interpretation of the behavior of CC-1065 and the duocarmycins (D. L. Boger, et al., *Angew. Chem., Int. Ed. Engl.* **1996**, *35*, 1439; and D. L. Boger, et al., *Chem. Rev.* **1997**, *97*, 787). First, the majority of the efficiency distinctions observed between the simple alkylation subunits such as **16**, **35**, and **36** and the natural products (10^3x of the 10^4x difference) may be attributed to ineffective catalysis of the DNA alkylation reaction with **16** and related agents and not their intrinsic capabilities or reversibility (kinetic effect) (D. L. Boger, et al., *J. Am. Chem. Soc.* **1994**, *116*, 1635; and D. L. Boger, *J. Am. Chem. Soc.* **1993**, *115*, 9872). The remaining 10-fold difference may be attributed to differences in the noncovalent binding affinity and/or the minor groove positioning and orientation of the agents consistent with identical conclusions drawn from the results of unrelated studies (D. L. Boger, et al., *J. Am. Chem. Soc.* **1997**, *119*, 4977; D. L. Boger, et al., *J. Am. Chem. Soc.* **1997**, *119*, 4987). Accordingly, **16**, **35**, and **36** appear to lack the structural features required for catalysis derived from a DNA binding induced conformational change in the natural products which disrupts the cross conjugated and stabilizing alkylation subunit vinylogous amide activating them for nucleophilic attack (D. L. Boger, et al., *Bioorg. Med. Chem.* **1997**, *5*, 263; and D. L. Boger, *Acc. Chem. Res.* **1999**, *32*, 1043). Secondly, studies with more advanced CPyI analogues related to the structures of CC-1065 and the duocarmycins, like those with **16** illustrated in Figure 21, have shown that the DNA alkylation selectivity is unaffected by the metal cation catalysis. This indicates that the source of the alkylation selectivity is not uniquely embedded in the catalysis source which is consistent with proposals that it is derived from the compounds' noncovalent binding selectivity (D. L. Boger, et al., *Bioorg. Med. Chem.* **1994**, *2*, 115).

Other examples of metal cation initiation of a DNA alkylation reaction are unknown and, as such, the studies detailed herein appear to constitute the first

example. Intriguingly, comparative trace metal analysis of cancerous and noncancerous human tissues have revealed significant distinctions (I. L. Mulay, et al., *J. Natl. Cancer Inst.* **1971**, *47*, 1). Although no generalizations were possible across all tumor types, within a given tumor type these were significant and potentially exploitable differences. For example, Zn was found in breast carcinoma at levels 700% higher than in normal cells of the same type, while lung carcinoma exhibited a reversed and even larger 10-fold difference. Thus, chemotherapeutic agents subject to Zn activation exhibit an enhanced activity against breast carcinoma attributable to this difference in Zn levels. Such therapeutic applications of this class of agents complement their use as research tools and as models to probe the source of the duocarmycin and CC-1065 DNA alkylation selectivity and catalysis.

Synthetic Protocols

3-Bromo-8-hydroxy-6-nitroquinoline (5). A solution of 2-bromoacrolein (5.0 g, 37 mmol, 1.0 equiv) in glacial acetic acid (110 mL) at 25 °C was titrated to the appearance of a faint redish color with bromine (ca. 5.9 g, 37 mmol, 1.0 equiv). 2-Hydroxy-4-nitroaniline (**4**, 5.7 g, 37 mmol, 1.0 equiv) was added, and the solution was gradually heated to 100 °C. The solution was cooled to 25 °C after 1 h. Filtering and neutralization of the precipitate with sodium phosphate buffer (1 M, pH 7, Na_2HPO_4-NaH_2PO_4) afforded 9.2 g (92%) of **5** as a light yellow solid: mp 240-241 °C; IR (film) ν_{max} 3408 (br), 3089, 1587 cm^{-1}. Anal. Calcd for $C_9H_5BrN_2O_3$: C, 40.18; H, 1.87; N, 10.41. Found: C, 40.21; H, 1.91; N, 9.98.

8-(Benzyloxy)-3-bromo-6-nitroquinoline (6). A solution of **5** (13.7 g, 51.0 mmol, 1.0 equiv) in anhydrous DMF (150 mL) was cooled to 4 °C under N_2 and treated with KI (1.70 g, 10.0 mmol, 0.2 equiv) and NaH (60% dispersion in oil, 2.24 g, 56.0 mmol, 1.1 equiv). Benzyl bromide (7.30 mL, 6.10 mmol, 1.2 equiv) was added after 30 min and the reaction was allowed to warm to 25 °C. After 24 h, the reaction volume was reduced by two-thirds *in vacuo* and EtOAc (200 mL) was added. The reaction mixture was poured on H_2O (200 mL) and extracted with EtOAc (3 x 100 mL). The combined organic extracts were washed with saturated

aqueous NaCl (40 mL), dried (Na_2SO_4) and concentrated. Flash chromatography (SiO_2, 5.5 × 20 cm, 50-100% CH_2Cl_2-hexane gradient) afforded **6** (15.6 g, 85%) as a yellow solid: mp 170 °C; FABHRMS (NBA/NaI) *m/z* 359.0040 (M + H^+, $C_{16}H_{11}BrN_2O_3$ requires 359.0031). Anal. Calcd for $C_{16}H_{11}BrN_2O_3$: C, 53.50; H, 3.09; N, 7.80. Found: C, 53.81; H, 3.23; N, 7.48.

8-(Benzyloxy)-3-bromo-6-(*N*-(*tert*-butyloxycarbonyl))aminoquinoline (7). A solution of **6** (0.20 g, 0.56 mmol, 1.0 equiv) in EtOAc (1.1 mL) at 25 °C was treated with $SnCl_2{\cdot}2H_2O$ (0.63 g, 2.8 mmol, 5.0 equiv). The reaction mixture was heated to 70 °C under N_2 until an orange slurry formed (ca. 0.5 h). After cooling to 25 °C, the reaction mixture was poured on ice and neutralized with 1 N aqueous NaOH. The aqueous layer was extracted with EtOAc (3 × 15 mL) and the combined organic layers were filtered, washed with saturated aqueous NaCl (10 mL), dried (Na_2SO_4) and concentrated. The yellow solid was placed under vacuum for 0.5 h and then dissolved in anhydrous dioxane (5.0 mL) and treated with di-*tert*-butyl dicarbonate (0.49 g, 2.3 mmol, 4.0 equiv) and Et_3N (0.16 mL, 1.1 mmol, 2.0 equiv). The reaction mixture was warmed to 70 °C under Ar for 1 d. After cooling to 25 °C, the solvent was removed *in vacuo*. Chromatography (SiO_2, 3 × 13 cm, 25% EtOAc-hexane) afforded **7** (0.18 g, 74%) as a light yellow solid: mp 162 °C; IR (film) ν_{max} 3354, 2971, 2919, 1807, 1766, 1724 cm^{-1}; FABHRMS (NBA/CsI) *m/z* 429.0825 (M + H^+, $C_{21}H_{21}BrN_2O_3$ requires 429.0814).

***n*-Butyl 8-(Benzyloxy)-6-(*N*-(*tert*-butyloxycarbonyl)amino)quinoline-3-carboxylate (8).** A solution of **7** (4.4 g, 10 mmol, 1.0 equiv) in *n*-BuOH (85 mL) was degassed with N_2. $Pd(PPh_3)_4$ (1.2 g, 1.0 mmol, 0.1 equiv) and *n*-Bu_3N (2.9 mL, 12 mmol, 1.2 equiv) were added and the solution was again purged with N_2. The reaction mixture was flushed with CO and then slowly heated to 100 °C under a CO atmosphere. Upon complete reaction (ca. 12 h), H_2O (50 mL) and saturated aqueous NH_4Cl (50 mL) were added. The organic layer was separated and the aqueous layer was extracted with EtOAc (3 × 50 mL). The combined organic layers were washed with saturated aqueous NaCl (40 mL), dried (Na_2SO_4) and concentrated. Chromatography (SiO_2, 5.5 × 20 cm, 25% EtOAc-hexane) afforded **8** (3.6 g, 78%) as a yellow solid: mp 135-136 °C; FABHRMS (NBA/CsI) *m/z* 451.2249 (M + H^+, $C_{26}H_{30}N_2O_5$ requires 451.2233).

Methyl 8-(Benzyloxy)-6-(*N*-(*tert*-butyloxycarbonyl)amino)quinoline-

3-carboxylate (9). A solution of **8** (2.9 g, 6.4 mmol, 1.0 equiv) in CH_3OH (70 mL) was cooled to 4 °C under N_2 and treated with LiOMe (0.28 g, 7.1 mmol, 1.1 equiv). The reaction mixture was allowed to warm to 25 °C after 20 min. Upon complete reaction (ca. 1.5 h), H_2O (100 mL) was added. The organic layer was separated and the aqueous layer was extracted with EtOAc (3 × 30 mL). The organic layers were combined, washed with saturated aqueous NaCl (30 mL), dried (Na_2SO_4) and concentrated. Chromatography (SiO_2, 5 × 19 cm, 25-30% EtOAc-hexane gradient) afforded **9** (2.4 g, 91%) as a yellow solid: mp 173-174 °C; FABHRMS (NBA/CsI) *m/z* 409.1773 (M + H^+, $C_{23}H_{24}N_2O_5$ requires 409.1763). Anal. Calcd for $C_{23}H_{24}N_2O_5$: C, 67.63; H, 5.92; N, 6.86. Found: C, 68.00; H, 5.98; N, 6.75.

Methyl 8-(Benzyloxy)-6-(*N*-(*tert*-butyloxycarbonyl)amino)-5-iodoquinoline-3-carboxylate (10). A solution of **9** (2.1 g, 5.2 mmol, 1.0 equiv) in a 1:1 mixture of THF-CH_3OH (85 mL) was cooled to 4 °C and treated with catalytic TsOH (40 mg) in THF (0.5 mL). *N*-Iodosuccinimide (1.4 g, 6.2 mmol, 1.2 equiv) in THF (10 mL) was slowly added over 10 min. After 1.5 h, the reaction mixture was warmed to 25 °C and stirred 45 h. Upon complete reaction, saturated aqueous $NaHCO_3$ (100 mL), Et_2O (100 mL), and 100 mL H_2O (100 mL) were added. The organic layer was separated and the aqueous layer was extracted with Et_2O (3 × 50 mL) and EtOAc (50 mL). The organic layers were combined, washed with saturated aqueous $NaHCO_3$ (50 mL) and saturated aqueous NaCl (50 mL), dried (Na_2SO_4) and concentrated. Chromatography (SiO_2, 5 × 19 cm, hexanes then 30% EtOAc-hexane) provided **10** (2.3 g, 84%, typically 80-88%) as a yellow solid: mp 182-183 °C; FABHRMS (NBA/CsI) *m/z* 535.0743 (M + H^+, $C_{23}H_{23}IN_2O_5$ requires 535.0730).

Methyl 8-(Benzyloxy)-6-[(*N*-(*tert*-butyloxycarbonyl)-*N*-(2-propenyl))amino]-5-iodo- quinoline-3-carboxylate (11). A solution of **10** (0.40 g, 0.75 mmol, 1.0 equiv) in anhydrous DMF (6.2 mL) at 4 °C in a flamed dried round bottom flask was treated with NaH (60% dispersion in oil, 33 mg, 0.82 mmol, 1.1 equiv) and stirred under Ar. After 30 min, allyl bromide (94 µL, 2.3 mmol, 3.0 equiv) was added and the reaction mixture was warmed to 25 °C and stirred 2.5 h. Saturated aqueous $NaHCO_3$ (1.5 mL) and EtOAc (5 mL) were added and the reaction was then poured on H_2O (100 mL). The aqueous layer was extracted

with EtOAc (4 × 20 mL) and the combined organic extract was washed with H_2O (2 × 40 mL) and saturated aqueous NaCl (2 × 40 mL), dried (Na_2SO_4), and concentrated *in vacuo*. Chromatography (SiO_2, 2.5 × 16 cm, 20-25% EtOAc-hexane gradient) afforded **11** (0.40 g, 94%) as a gold solid (mixture of amide rotamers in $CDCl_3$): mp 128-129 °C; FABHRMS (NBA/CsI) *m/z* 575.1036 (M + H^+, $C_{26}H_{27}IN_2O_5$ requires 575.1043).

Methyl 5-(Benzyloxy)-3-(*tert*-butyloxycarbonyl)-1-[[(2',2',6',6'-tetramethyl piperidino)-oxy]methyl]-1,2-dihydro-3*H*-pyrido[3,2-*e*]indole-8-carboxylate (12). A solution of **11** (20 mg, 35 µmmol, 1.0 equiv) in anhydrous toluene (1.2 mL) was treated with a solution of TEMPO (16 mg, 0.11 mmol, 3.0 equiv) in toluene (0.11 mL) and $(TMS)_3SiH$ (11 µL, 37 µmol, 1.05 equiv). The solution was warmed to 80 °C and 5 equiv of TEMPO (2 × 14 mg in 0.29 mL toluene) and 4 equiv $(TMS)_3SiH$ (4 × 11 µL) were added in portions over the next 4 h. After 16 h, the reaction mixture was cooled to 25 °C and the volatiles removed *in vacuo*. Chromatography (SiO_2, 1.5 × 12 cm, 20% EtOAc-hexane) provided **12** (18 mg, 85%) as a gold solid: mp 157-158 °C; FABHRMS (NBA/CsI) *m/z* 726.2383 (M + Cs^+, $C_{35}H_{45}N_3O_5$ requires 736.2363). Anal. Calcd. for $C_{35}H_{45}N_3O_5 \cdot H_2O$: C, 67.61; H, 7.62; N, 6.76. Found: C, 67.70; H, 7.11; N, 6.27.

Methyl 5-(Benzyloxy)-3-(*tert*-butyloxycarbonyl)-1-(hydroxymethyl)-1,2-dihydro-3*H*- pyrido[3,2-*e*]indole-8-carboxylate (13). A solution of **12** (20 mg, 33 µmol, 1.0 equiv) in a 3:1 mixture of THF-H_2O (0.90 mL) was treated with activated zinc powder (54 mg, 0.80 mmol, 25 equiv) and HOAc (0.20 mL) and the resulting suspension was warmed to 60 °C with vigorous stirring. After 7 h, additional Zn (54 mg) was added and the reaction was stirred 4 h. The Zn powder was removed by filtration through Celite with a CH_2Cl_2 wash (10 mL), and the mixture was concentrated *in vacuo*. The resulting residue was dissolved in EtOAc (10 mL), filtered through Celite, and the solution was concentrated *in vacuo*. Chromatography (SiO_2, 1 × 12 cm, 20-50% EtOAc-hexane) provided **13** (9.2 mg, 60%): mp 186 °C; FABHRMS (NBA/CsI) *m/z* 465.2032 (M + H^+, $C_{26}H_{28}N_2O_5$ requires 465.2026).

Methyl 5-(Benzyloxy)-3-(*tert*-butyloxycarbonyl)-1-(chloromethyl)-1,2-dihydro-3*H* -pyrido[3,2-*e*]indole-8-carboxylate (14). Method A: A solution of **13** (6.7 mg, 14

μmol, 1.0 equiv) in anhydrous CH_2Cl_2 (0.14 mL) under Ar was treated sequentially with Ph_3P (13 mg, 48 μmol, 3.0 equiv) and CCl_4 (14 μL, 0.15 mmol, 9.0 equiv). The reaction mixture was stirred at 25 °C for 3 h. The solvent was then evaporated under a stream of N_2. Radial chromatography (SiO_2, 1.0 mm, 20% EtOAc-hexane) afforded **14** (5.1 mg, 73%) as a gold solid: mp 194 °C (EtOAc-hexane); FABHRMS (NBA/NaI) *m/z* 483.1675 (M + H^+, $C_{26}H_{27}ClN_2O_5$ requires 483.1687). Anal. Calcd for $C_{26}H_{27}ClN_2O_5$: C, 64.66; H, 5.63; N, 5.80. Found: C, 64.78; H, 5.73; N, 5.66.

Methyl 3-(*tert*-Butyloxycarbonyl)-1-(chloromethyl)-5-hydroxy-1,2-dihydro-3*H*-pyrido[3,2-e]indole-8-carboxylate (15). A slurry of **14** (0.9 g, 1.9 mmol, 1.0 equiv) and 10% Pd-C (0.36 g) in THF (6.2 mL) under N_2 was cooled to -78 °C and degassed under vacuum. The reaction was warmed to 25 °C and treated with 25% aqueous HCO_2NH_4 (1.2 g in 4.7 mL H_2O, 19 mmol, 10 equiv). After 3 h, the catalyst was removed by filtration through Celite (2 × 50 mL Et_2O wash) and the solvent was evaporated under reduced pressure to afford **15** (0.72 g, 99%) as a bright yellow solid: mp 162-163 °C; FABHRMS (NBA/NaI) *m/z* 393.1228 (M + H^+, $C_{18}H_{21}ClN_2O_5$ requires 393.1217).

Methyl 2-(*tert*-Butyloxycarbonyl)-1,2,9,9a-tetrahydrocyclopropa[*c*]pyrido[3,2-*e*]indol- 4-one-7-carboxylate (16, *N*-BOC-CPyI). A solution of **15** (81 mg, 0.21 mmol, 1.0 equiv) in CH_3CN (6.9 mL) at 25 °C under Ar was treated with DBU (0.12 mL, 0.83 mmol, 4.0 equiv) and stirred 3 h. Flash chromatography was applied directly to the reaction mixture (SiO_2, 2.5 × 8 cm, 2% MeOH-CH_2Cl_2) and furnished **16** as a light yellow-white solid (68 mg, 93%, typically 90-99%): mp 255 °C (dec); IR (film) ν_{max} 2974, 1728 cm^{-1}; UV (CH_3OH) λ_{max} 318 (ε = 9000), 240 (shoulder, ε = 11000), 218 (ε = 15500); FABHRMS (NBA/NaI) *m/z* 379.1282 (M + Na^+, $C_{18}H_{20}N_2O_5$ requires 379.1270).

Resolution of *N*-BOC-CPyI. Samples of racemic **16** were resolved by semi-preparative HPLC chromatography on a Daicel ChiralCel OD column (10 μm, 2 × 25 cm) using 50% *i*-PrOH-hexane eluant (7 mL/min). The enantiomers eluted with retention times of 27.3 min and 37.8 min (α = 1.43). (+)-(8b*R*, 9a*S*)-**16**: $[\alpha]^{22}_D$ +120 (*c* 0.46, THF); (-)-(8b*S*, 9a*R*)-**16**: -118 (*c* 0.47, THF).

Methyl 1,2,9,9a-Tetrahydrocyclopropa[*c*]pyrido[3,2-*e*]indol-4-one-7-carboxylate (17, CPyI). A solution of **16** (4.0 mg, 11 μmol, 1.0 equiv) in 3 M

HCl-EtOAc (0.37 mL) was stirred for 30 min at 25 °C. The solvent was removed by a stream of N_2 and the residual salt was dried under vacuum. The residue was taken up in acetone (0.28 mL) and treated with K_2CO_3 (16 mg, 0.11 mmol, 10 equiv). After stirring for 24 h at 25 °C, the reaction mixture was filtered through Celite to provide **17** as a yellow solid film (2.7 mg, 96%): UV (CH_3OH) λ_{max} 360 (ε = 7000), 298 (shoulder, ε = 5000), 226 (ε = 15000); FABHRMS (NBA/NaI) *m/z* 257.0927 (M + H^+, $C_{14}H_{12}N_2O_3$ requires 257.0926); (+)-(8b*R*, 9a*S*)-**17**: $[\alpha]^{22}_D$ +41 (*c* 0.14, CH_2Cl_2); (-)-(8b*S*, 9a*R*)-**17**: -45 (*c* 0.09, CH_2Cl_2).

Methyl 8-(Benzyloxy)-6-[(*N*-(*tert*-butyloxycarbonyl)-*N*-(*E*-3-chloro-2-propenyl))- amino]-5-iodoquinoline-3-carboxylate (18). A solution of **10** (1.2 g, 2.2 mmol, 1.0 equiv) in anhydrous DMF (20 mL) was cooled to 4 °C in a flamed dried round bottom flask under Ar and was treated with NaH (60% dispersion in oil, 98 mg, 2.5 mmol, 1.1 equiv). After 30 min, *E*-1,3-dichloropropene (0.61 mL, 6.7 mmol, 3.0 equiv) was added and the reaction mixture was gradually warmed to 25 °C and stirred 12 h. The reaction was poured on H_2O (100 mL) and saturated aqueous $NaHCO_3$ (50 mL). The aqueous layer was extracted with EtOAc (4 × 50 mL) and the combined organic extract was washed with saturated aqueous $NaHCO_3$ (50 mL), H_2O (2 × 40 mL), and saturated aqueous NaCl (2 × 40 mL), dried (Na_2SO_4), and concentrated *in vacuo*. Chromatography (SiO_2, 5.5 × 14 cm, 20-30% EtOAc-hexane gradient) afforded **18** (1.2 g, 85%, typically 84-94%) as a yellow foam (mixture of amide rotamers in $CDCl_3$). FABHRMS (NBA/CsI) *m/z* 740.9646 (M + Cs^+, $C_{26}H_{28}ClN_2O_5I$ requires 740.9629).

Methyl 5-(Benzyloxy)-3-(*tert*-butyloxycarbonyl)-1-(chloromethyl)-1,2-dihydro-3*H*- pyrido[3,2-*e*]indole-8-carboxylate (14). Method B: A solution of **18** (0.65 g, 1.1 mmol, 1.0 equiv) in benzene (20 mL) under Ar was treated with *n*-$BuSn_3H$ (0.15 mL, 0.50 mmol, 0.5 equiv) and catalytic AIBN (18 mg) and stirred at 70 °C. Additional *n*-$BuSn_3H$ (0.29 mL, 1.1 mmol, 1.0 equiv in 2 portions) was added over the next hour. After 3 h, the reaction mixture was concentrated *in vacuo*. Chromatography (SiO_2, 4 x 20 cm, 20-30% EtOAc-hexane gradient) provided **14** (0.46 g, 87%).

Methyl 1-(Chloromethyl)-5-hydroxy-3-[(5,6,7-trimethoxyindol-2-yl) carbonyl]-1,2- dihydro-3*H*-pyrido[3,2-*e*]indole-8-carboxylate (*seco*-CPyI-TMI, 24). A solution of **16** (10.0 mg, 28.1 µmol, 1.0 equiv) in 3 M HCl-EtOAc (0.935

mL) was stirred for 30 min at 25 °C. The solvent was removed by a stream of N_2 and the residual salt was dried under vacuum. The residue was dissolved in anhydrous DMF (0.300 mL) and treated with 5,6,7-trimethoxyindole-2-carboxylic acid (**19**, 10.6 mg, 42.1 µmol, 1.5 equiv) and EDCI (27.0 mg, 140 µmol, 5.0 equiv). After stirring for 10 h at 25 °C under Ar, the reaction mixture was concentrated *in vacuo* and suspended in H_2O. The precipitate was collected by centrifugation and washed with H_2O (4 mL). Flash chromatography (SiO_2, 0.7 × 7 cm, 1-5% MeOH-$CHCl_3$ gradient) afforded **24** (7.7 mg, 52%) as a light yellow solid: FABHRMS (NBA/CsI) *m/z* 526.1397 (M + H^+, $C_{28}H_{24}ClN_3O_7Cl$ requires 526.1381); (+)-(1*S*)-**24**: $[\alpha]^{25}_D$ +6 (*c* 0.33, $CHCl_3$); (-)-(1*R*)-**24**: $[\alpha]^{25}_D$-6 (*c* 0.33, $CHCl_3$).

Methyl 2-[(5,6,7-Trimethoxyindol-2-yl)carbonyl]-1,2,9,9a-tetrahydrocyclopropa[*c*]-pyrido[3,2-*e*]indol-4-one-7-carboxylate (25, CPyl-TMI). A solution of **24** (1.5 mg, 2.8 µmol, 1.0 equiv) in anhydrous DMF (0.10 mL) at 25 °C was treated with DBU (1.3 µL, 8.6 µmol, 3.0 equiv) and stirred 3 h under Ar. Direct chromatography of the reaction mixture (0.7 × 3 cm, 5% MeOH-CH_2Cl_2) furnished **25** as a light yellow solid (1.2 mg, 86%): FABHRMS (NBA/NaI) *m/z* 490.1629 (M + H^+, $C_{28}H_{23}N_3O_7$ requires 490.1614); (+)-(8b*R*, 9a*S*)-**25**: $[\alpha]^{25}_D$ +42 (*c* 0.085, CH_2Cl_2); (-)-(8b*S*, 9a*R*)-**25**: $[\alpha]^{25}_D$ -44 (*c* 0.045, CH_2Cl_2).

Methyl 1-(Chloromethyl)-5-hydroxy-3-[(5-methoxyindol-2-yl)carbonyl]-1,2-dihydro- 3*H*-pyrido[3,2-*e*]indole-8-carboxylate (26). Flash chromatography (SiO_2, 0.7 × 6 cm, 1-5% MeOH-$CHCl_3$ gradient) afforded **26** (59%) as a yellow solid: FABHRMS (NBA/NaI) *m/z* 466.1186 (M + H^+, $C_{24}H_{20}ClN_3O_5$ requires 466.1170); (+)-(1*S*)-**26**: $[\alpha]^{25}_D$ +13 (*c* 0.16, $CHCl_3$); (-)-(1*R*)-**26**: $[\alpha]^{25}_D$-12 (*c* 0.27, $CHCl_3$).

Methyl 2-[(5-Methoxyindol-2-yl)carbonyl]-1,2,9,9a-tetrahydrocyclopropa-[*c*]pyrido[3,2-*e*]indol-4-one-7-carboxylate (27). Flash chromatography (0.7 × 3 cm, 5% MeOH-CH_2Cl_2) furnished **27** as a light yellow solid (90%): FABHRMS (NBA/NaI) *m/z* 452.1209 (M + Na^+, $C_{24}H_{19}N_3O_5$ requires 452.1222); (+)-(8b*R*, 9a*S*)-**27**: $[\alpha]^{25}_D$ +49 (*c* 0.07, CH_2Cl_2); (-)-(8b*S*, 9a*R*)-**27**: $[\alpha]^{25}_D$ -44 (*c* 0.055, CH_2Cl_2).

Methyl 1-(Chloromethyl)-5-hydroxy-3-[(indol-2-yl)carbonyl]-1,2-dihydro-3*H*-

pyrido[3,2-e]indole-8-carboxylate (*seco*-CPyI-indole, 28). Flash chromatography (SiO_2, 0.7 × 7 cm, 1-5% MeOH-$CHCl_3$ gradient) afforded **28** (71%) as a yellow solid: FABHRMS (NBA/NaI) *m/z* 436.1052 (M + H^+, $C_{23}H_{18}ClN_3O_4I$ requires 436.1064); (+)-(1*S*)-**28**: $[\alpha]^{25}_D$ +3 (*c* 0.35, $CHCl_3$); (-)-(1*R*)-**28**: $[\alpha]^{25}_D$-3 (*c* 0.29, $CHCl_3$).

Methyl 2-[(Indol-2-yl)carbonyl]-1,2,9,9a-tetrahydrocyclopropa[*c*]pyrido [3,2-*e*]indol- 4-one-7-carboxylate (CPyI-indole, 29). Flash chromatography (0.7 × 3 cm, 5% MeOH-CH_2Cl_2) furnished **29** as a light yellow solid (93%): FABHRMS (NBA/NaI) *m/z* 400.1310 (M + H^+, $C_{23}H_{17}N_3O_4$ requires 400.1297); (+)-(8b*R*, 9a*S*)-**29**: $[\alpha]^{25}_D$ +48 (*c* 0.065, CH_2Cl_2); (-)-(8b*S*, 9a*R*)-**29**: $[\alpha]^{25}_D$ -43 (*c* 0.065, CH_2Cl_2).

Methyl 1-(Chloromethyl)-5-hydroxy-3-{[5-[N-(indol-2-yl)carbonyl] aminoindol-2-yl]-carbonyl}-1,2-dihydro-3*H*-pyrido[3,2-e]indole-8-carboxylate (*seco*-CPyI-indole$_2$, 30). Flash chromatography (SiO_2, 0.7 × 6 cm, 10% DMF-$CHCl_3$) afforded **30** (64%) as a yellow solid: FABHRMS (NBA/CsI) *m/z* 726.0548 (M + Cs^+, $C_{32}H_{24}ClN_5O_5$ requires 726.0520); (+)-(1*S*)-**30**: $[\alpha]^{25}_D$ +26 (*c* 0.105, DMF); (-)-(1*R*)-**30**: $[\alpha]^{25}_D$-28 (*c* 0.06, DMF).

Methyl 2-{[5-[N-(Indol-2-yl)carbonyl]aminoindol-2-yl]carbonyl}-1,2,9,9a-tetrahydrocyclopropa[*c*]pyrido[3,2-*e*]indol-4-one-7-carboxylate (CPyI-indole$_2$, 31). Flash chromatography (SiO_2, 0.7 × 2 cm, 10% DMF-CH_2Cl_2) afforded **31** (97%) as a yellow solid: MALDIHRMS (DHB) *m/z* 558.1757 (M + H^+, $C_{32}H_{23}ClN_5O_5$ requires 558.1778); (+)-(1*S*)-**31**: $[\alpha]^{25}_D$ +50 (*c* 0.04, DMF); (-)-(1*R*)-**31**: $[\alpha]^{25}_D$-46 (*c* 0.05, DMF).

Methyl 3-[(3-Carbamoyl-1,2-dihydro-3*H*-pyrrolo[3,2-e]indol-7-yl)carbonyl]-1-(chloromethyl)-5-hydroxy-1,2-dihydro-3*H*-pyrido[3,2-e]indole-8-carboxylate (*seco*-CPyI-CDPI$_1$, 32). Flash chromatography (SiO_2, 0.7 × 7 cm, 5% MeOH-10% DMF-$CHCl_3$) afforded **32** (41%) as a yellow solid: MALDIHRMS (DHB) *m/z* 520.1383 (M + H^+, $C_{26}H_{22}ClN_5O_5$ requires 520.1388); (+)-(1*S*)-**32**: $[\alpha]^{25}_D$ +23 (*c* 0.04, DMF); (-)-(1*R*)-**32**: $[\alpha]^{25}_D$-20 (*c* 0.06, DMF).

Methyl 2-[(3-Carbamoyl-1,2-dihydro-3*H*-pyrrolo[3,2-e]indol-7-yl)carbonyl]-1,2,9,9a- tetrahydrocyclopropa[*c*]pyrido[3,2-*e*]indol-4-one-7-carboxylate (CPyI-CDPI$_1$, 33). Flash chromatography (SiO_2, 0.7 × 4 cm, 5% MeOH-10% DMF-CH_2Cl_2) afforded **33** (67%) as a yellow solid: MALDIHRMS (DHB) *m/z*

484.1613 (M + H$^+$, $C_{26}H_{21}N_5O_5$ requires 484.1621); (+)-(1*S*)-**33**: $[\alpha]^{25}_D$ +50 (*c* 0.03, DMF); (-)-(1*R*)-**33**: $[\alpha]^{25}_D$-53 (*c* 0.03, DMF).

Aqueous Solvolysis of *N*-BOC-CPyl and CPyl (pH 2 and pH 3, phosphate buffer). Samples of **16** (0.15 mg) and **17** (0.05 mg) were dissolved in CH_3OH (1.5 mL) and mixed with pH 3.0 buffer (1.5 mL, 4:1:20 (v:v:v) 0.1 M citric acid, 0.2 M Na_2HPO_4, and H_2O, respectively). Similarly, samples of **16** (0.1 mg) and **17** (0.05 mg) were dissolved in CH_3OH (1.5 mL) and mixed with pH 2.0 buffer (1.5 mL, 4:1:20 (v:v:v) 1.0 M citric acid, 0.2 M Na_2HPO_4, and H_2O, respectively). After mixing, the UV spectra of the solution was measured against a reference solution containing CH_3OH (1.5 mL) and the appropriate aqueous buffer (1.5 mL) and these readings were used for the initial absorbance values (A_i). The UV spectrum was measured at regular intervals for 30 d (**16** at pH 3), 14 d (**16** at pH 2), 40 d (**17** at pH 3), and 8 d (**17** at pH 2). For **16**, the decrease in the long-wavelength absorption at 315 nm and increase in the short-wavelength absorption at 278 nm were monitored. The solvolysis rate constant and half-life (pH 3: $k = 3.81 \times 10^{-6}$ s^{-1}, $t_{1/2}$ = 51 h, r = 0.99; pH 2: $k = 3.72 \times 10^{-5}$ s^{-1}, $t_{1/2}$ = 5.2 h, r = 0.99) were calculated from the least-squares treatment of the slope of the plot of time versus $\ln[(A_f - A_i)/(A_f - A)]$ (Figure 10). For **17**, the decrease in the long-wavelength absorption at 362 nm and increase in the short-wavelength absorption at 290 nm were monitored. The solvolysis rate constant and half-life were calculated by the same treatment providing $k = 6.27 \times 10^{-7}$ s^{-1} ($t_{1/2}$ = 310 h, r = 0.99) for pH 3 and $k = 4.63 \times 10^{-5}$ s^{-1} ($t_{1/2}$ = 42 h, r = 0.99) for pH 2.

Acid-Catalyzed Addition of CH_3OH to *N*-BOC-CPyl: Methyl 3-(*tert*-butyloxycarbonyl)-5-hydroxy-1-(methoxymethyl)-1,2-dihydro-3*H*-pyrido[3,2-e]indole-8- carboxylate (41). A solution of **16** (3.0 mg, 8.4 µmol, 1.0 equiv) in CH_3OH (0.43 mL) was treated with CF_3SO_3H (0.13 µL, 2.5 µmol, 0.3 equiv) at 25 °C. After 20 h, the reaction was quenched by the addition of $NaHCO_3$ (9 mg), filtered through Celite, and concentrated *in vacuo*. Chromatography (SiO_2, 0.7 × 7 cm, 5-50% EtOAc-$CHCl_3$ gradient) afforded **41** (3.0 mg, 91%) as a yellow solid: FABHRMS (NBA/NaI) *m/z* 389.1706 (M + H$^+$, $C_{20}H_{24}N_2O_6$ requires 389.1713).

Addition of HCl to *N*-BOC-CPyl. A solution of **16** (2.3 mg, 6.5 µmol, 1.0 equiv)

in THF (0.15 mL) was cooled to -78 °C and treated with 4 M HCl-EtOAc (3.0 µL, 11 µmol, 1.7 equiv). The mixture was stirred for 2 min before the solvent was removed *in vacuo*. Chromatography (SiO_2, 0.7 × 7 cm, 10% EtOAc-$CHCl_3$) afforded **15** (2.4 mg, 96%).

Aqueous Solvolysis of *N*-BOC-CPyl (pH 2-11, universal buffer). Samples of **16** (0.025 mg) were dissolved in CH_3OH (1.0 mL), and the resulting solutions were mixed with a universal aqueous buffer (Perrin, D. D.; Dempsey, B. *Buffers for pH and Metal Ion Control;* Chapman and Hall: London, 1979; p 156) (pH 2-11, 1.0 mL, $B(OH)_3$-citric acid-Na_3PO_4). After mixing, the UV spectra of the solution were measured against reference solutions and these readings were used for the initial absorbance values (A_i). The UV spectrum was measured at regular intervals (pH 2-4: every hour for 1d and then every 24 h; pH 4-10: every 24 h) until no further change in absorbance was observed (A_f). The decrease in the long-wavelength absorption at 320 nm and increase in the short-wavelength absorption at 278 nm were monitored. The solvolysis rate constants and half-lives were calculated from the least-squares treatment of the slope of the plot of time versus $\ln[(A_f - A_i)/(A_f - A)]$.

Lewis Acid-Catalyzed Addition of CH_3OH to *N*-BOC-CPyl. A solution of **16** (1.2 mg, 3.4 µmol, 1.0 equiv) in CH_3OH (0.14 mL) was treated with $Zn(OTf)_2$ (1.4 mg, 3.9 µmol, 1.1 equiv) at 25 °C. After 4 h, the solvent was removed with a stream of N_2. Flash chromatography (SiO_2, 0.7 × 7 cm, 20-50% EtOAc-$CHCl_3$ gradient) afforded **41** (1.2 mg, 92%).

Metal-Catalyzed Solvolysis of *N*-BOC-CPyl. Samples of **16** (0.025 mg) were dissolved in CH_3OH (1.9 mL) and the resulting solutions were treated with 125 µL (1.0 equiv) or 25 µL (0.2 equiv) of a 0.56 mM solution (CH_3OH) of the desired metal ($Cu(acac)_2$, Mg $(acac)_2$, $Ni(acac)_2$, $Zn(acac)_2$, $Mn(acac)_2$, $Mg(acac)_2$, $Fe(acac)_3$, $Cr(acac)_3$, $Zn(OTf)_2$, $Ti(O\textit{i}\text{-}Pr)_4$, or $Cu(OMe)_2$). The solvolysis solution was sealed and kept at 25 °C protected from light. After mixing, the UV spectra of the solution were measured against reference solutions and these readings were used for the initial absorbance values (A_i). The UV spectrum was measured at regular intervals until no further change in absorbance was observed (A_f). The decrease in the long-wavelength absorption at 330 nm and increase in the short-wavelength absorption at 270 nm were monitored. The solvolysis rate

constants and half-lives were calculated from the least-squares treatment of the slope of the plot of time versus $\ln[(A_f - A_i)/(A_f - A)]$.

What is claimed is:

1. A DNA alkylating agent represented by the following structure:

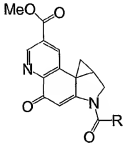

wherein **R** is a DNA minor groove binder.

2. A DNA alkylating agent according to claim 1 represented by the following structure:

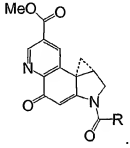

3. A DNA alkylating agent according to claim 2 wherein **R** is selected from a group of DNA minor groove binders represented by the following structures:

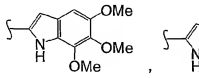
, 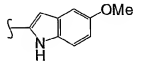
, 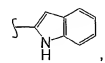
,

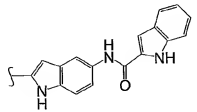
, and 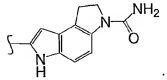
.

4. A DNA alkylating agent according to claim 3 represented by the following structure:

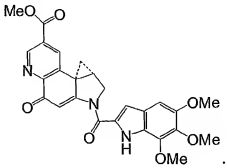

5. A DNA alkylating agent according to claim 3 represented by the following structure:

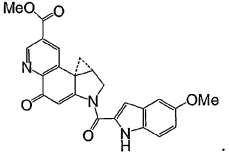

6. A DNA alkylating agent according to claim 3 represented by the following structure:

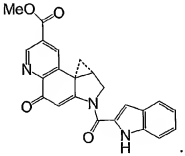

7. A DNA alkylating agent according to claim 3 represented by the following structure:

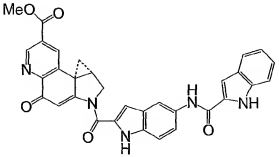

8. A DNA alkylating agent according to claim 3 represented by the following structure:

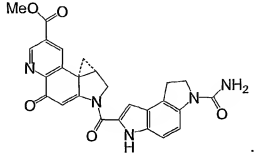

9. A DNA alkylating agent according to claim 1 represented by the following structure:

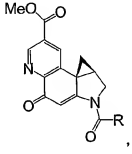

wherein **R** is selected from a group of DNA minor groove binders represented by the following structures:

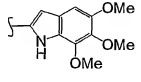

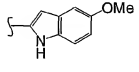

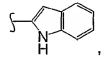

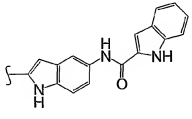

, and

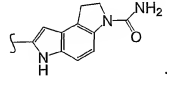

10. A DNA alkylating agent represented by the following structure:

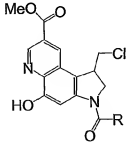

wherein **R** is a DNA minor groove binder.

11. A DNA alkylating agent according to claim 10 represented by the following structure:

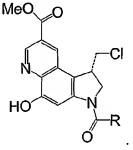

12. A DNA alkylating agent according to claim 11 wherein **R** is selected from a group of DNA minor groove binders represented by the following structures:

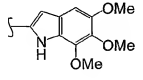
, 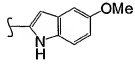
, 
,

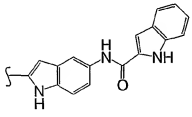
, and 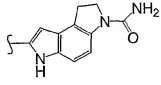
.

13. A DNA alkylating agent according to claim 12 represented by the following structure:

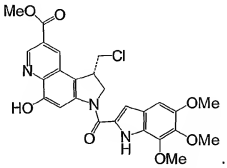

14. A DNA alkylating agent according to claim 12 represented by the following structure:

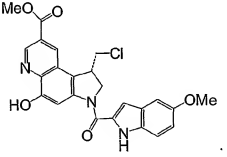

15. A DNA alkylating agent according to claim 12 represented by the following structure:

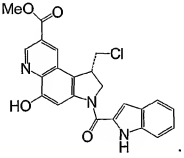

16. A DNA alkylating agent according to claim 12 represented by the following structure:

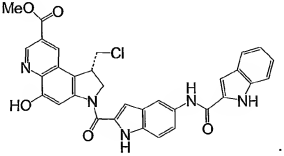

17. A DNA alkylating agent according to claim 12 represented by the following structure:

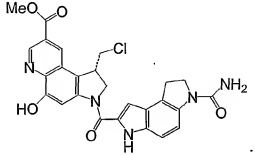

18. A DNA alkylating agent according to claim 13 represented by the following structure:

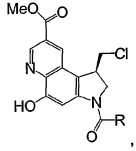

wherein **R** is selected from a group of DNA minor groove binders represented by the following structures:

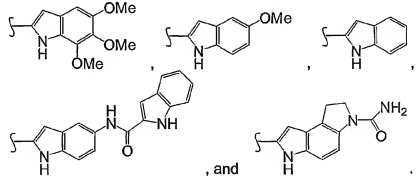

19. A process for catalyzing a solvolysis of a cyclopropyl ring of an N^2-derivative of methyl 1,2,9,9a-tetrahydrocyclopropa[*c*]pyrido[3,2-*e*]indol-4-one-7-carboxylate, the process comprising the following step:

contacting the N^2- derivative of methyl 1,2,9,9a-tetrahydrocyclopropa[*c*]pyrido[3,2-*e*]indol-4-one-7-carboxylate under

aqueous conditions having a pH greater than 4 with a catalytic concentration of a metal ion sufficient to catalyze the solvolysis of the cyclopropyl ring of the N^2- derivative of methyl 1,2,9,9a-tetrahydrocyclopropa[*c*]pyrido[3,2-*e*]indol-4-one-7-carboxylate, the metal ion being selected from a group consisting of Cu^{2+}, Ni^{2+}, Zn^{2+}, Cr^{2+}, Fe^{2+}, Cr^{3+}, Fe^{3+}, Mn^{2+}, and Mg^{2+}.

20. The process for catalyzing a solvolysis of the cyclopropyl ring of an N^2-derivative of methyl 1,2,9,9a-tetrahydrocyclopropa[*c*]pyrido[3,2-*e*]indol-4-one-7-carboxylate according to Claim 19 wherein the metal ion is Zn^{2+}.

21. A process for catalyzing the production of a DNA alkylation product, the process comprising the following step:

contacting DNA with an N^2- derivative of methyl 1,2,9,9a-tetrahydrocyclopropa[*c*]pyrido[3,2-*e*]indol-4-one-7-carboxylate under aqueous conditions having a pH greater than 4 in the presence of a catalytic concentration of metal ion sufficient to catalyze the alkylation of the DNA by the N^2- derivative of methyl 1,2,9,9a-tetrahydrocyclopropa[*c*]pyrido[3,2-*e*]indol-4-one-7-carboxylate for producing the DNA alkylation product, the metal ion being selected from a group consisting of Cu^{2+}, Ni^{2+}, Zn^{2+}, Cr^{2+}, Fe^{2+}, Cr^{3+}, Fe^{3+}, Mn^{2+}, and Mg^{2+}.

22. The process for catalyzing the production of a DNA alkylation product according to Claim 21 wherein the metal ion is Zn^{2+}.

23. A DNA alkylation product produced according to the method of claim 21.

24. A DNA alkylation product produced according to the method of claim 22.

22. A process for catalyzing cell death by DNA alkylation, the process

comprising the following step:

contacting a cell, under aqueous conditions having a pH greater than 4, with a concentration of an N^2- derivative of methyl 1,2,9,9a-tetrahydrocyclopropa[c]pyrido[3,2-e]indol-4-one-7-carboxylate sufficient, in the presence of a catalytic concentration of metal ion, to catalyze cell death by DNA alkylation, the metal ion being selected from a group consisting of Cu^{2+}, Ni^{2+}, Zn^{2+}, Cr^{2+}, Fe^{2+}, Cr^{3+}, Fe^{3+}, Mn^{2+}, and Mg^{2+}.

23. A process for catalyzing cell death by DNA alkylation according to Claim 22 wherein the metal ion is Zn^{2+}.

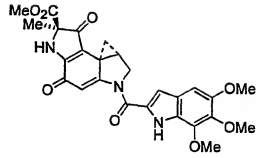

2, (+)-Duocarmycin A

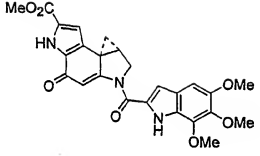

1, (+)-Duocarmycin SA

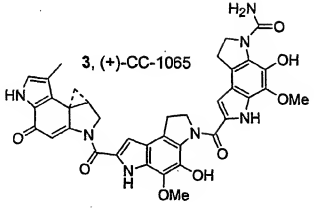

3, (+)-CC-1065

FIG. 1

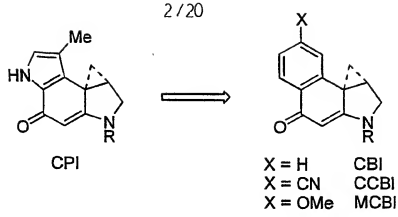
Me
HN
O
N
R
CPI
X
X = H CBI
X = CN CCBI
X = OMe MCBI

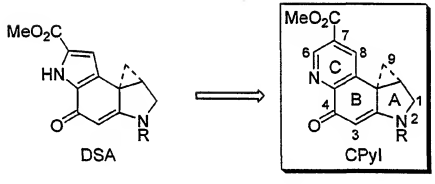
MeO2C
HN
O
N
R
DSA
MeO2C
7
6
8
9
N
C
B
A
1
4
N
2
3
O
R
CPyl

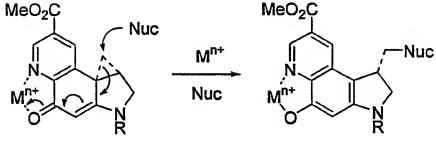
MeO2C
Nuc
N
Mn+
O
N
R
Mn+
Nuc
MeO2C
Nuc
N
Mn+
O
N
R

FIG. 2

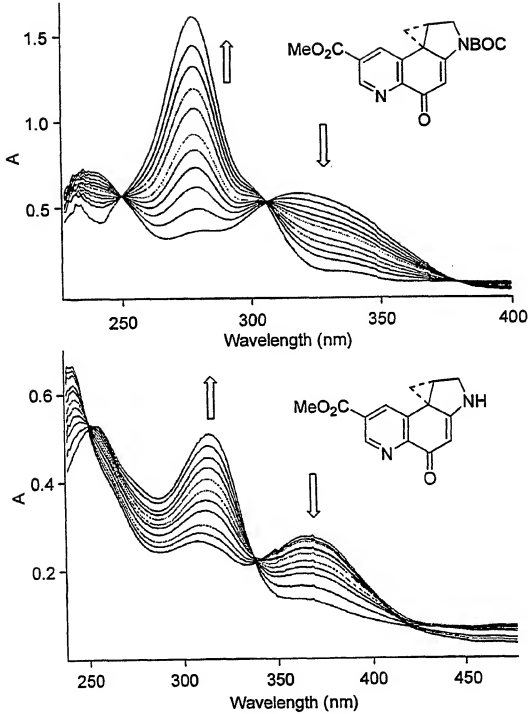

Solvolysis study (UV spectra) of *N*-BOC-CPyI (**16**, top) and CPyI (**17**, bottom) in 50% CH_3OH–aqueous buffer (pH 2, 4:1:20 (v:v:v) 1.0 M citric acid, 0.2 M NaH_2PO_4, and H_2O, respectively). The spectra were recorded at regular intervals, and only a few are shown for clarity. Top: (hours) 0, 1, 2, 3, 4, 5, 7, 9, 12, 16, 41. Bottom: (hours) 0, 5, 10, 20, 26, 35, 47, 66, 93, 144, 283.

FIG. 3

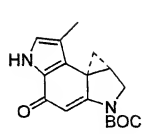

34, *N*-BOC-CPI

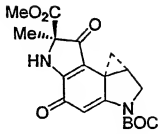

35, *N*-BOC-DA

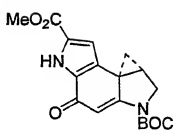

36, *N*-BOC-DSA

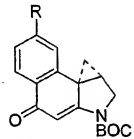

37, *N*-BOC-CBI R = H
38, *N*-BOC-MCBI R = OMe
39, *N*-BOC-CCBI R = CN

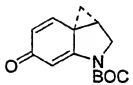

40, *N*-BOC-CI

Agent	k (s^{-1}, pH 3)	$t_{1/2}$ (h, pH 3)	Regioselectivity
16	3.81×10^{-6}	51	> 20 : 1
34	5.26×10^{-6}	37	4 : 1
35	1.75×10^{-5}	11	3 : 2
36	1.08×10^{-6}	177	6–4 : 1
37	1.45×10^{-6}	133	> 20 : 1
38	1.75×10^{-6}	110	> 20 : 1
39	0.99×10^{-6}	194	> 20 : 1
40	1.98×10^{-2}	0.01	nd

FIG. 4

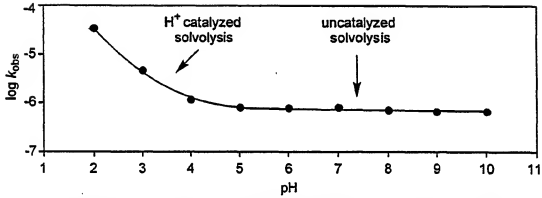

Plot of pH versus log k_{obs} for solvolysis of *N*-BOC-CPyI in universal buffer (pH 2–10).

FIG. 5

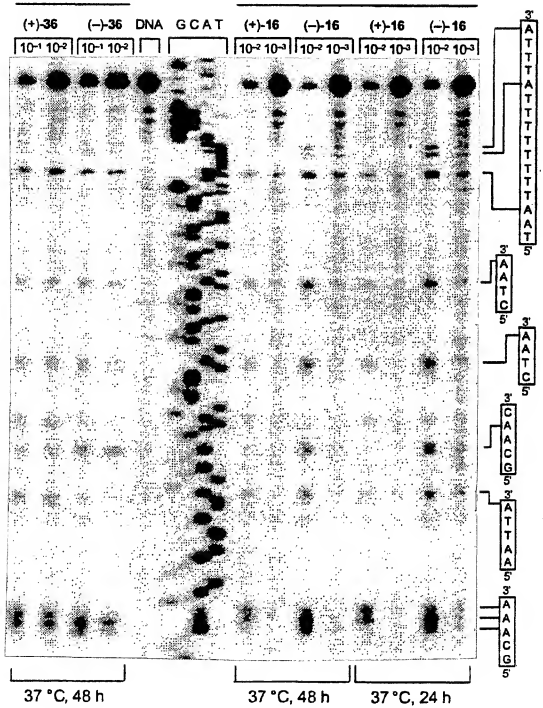
36: N-BOC-DSA
16: N-BOC-CPyl
(+)-36
(–)-36
DNA
G C A T
(+)-16
(–)-16
(+)-16
(–)-16
10⁻¹ 10⁻²
10⁻¹ 10⁻²
10⁻² 10⁻³
10⁻² 10⁻³
10⁻² 10⁻³
10⁻² 10⁻³
3' A T T T A T T T T T T T A A T 5'
3' A A T C 5'
3' A A T C 5'
3' C A A C G 5'
3' A T T A A 5'
3' A A A C G 5'
37 °C, 48 h
37 °C, 48 h
37 °C, 24 h

FIG. 6

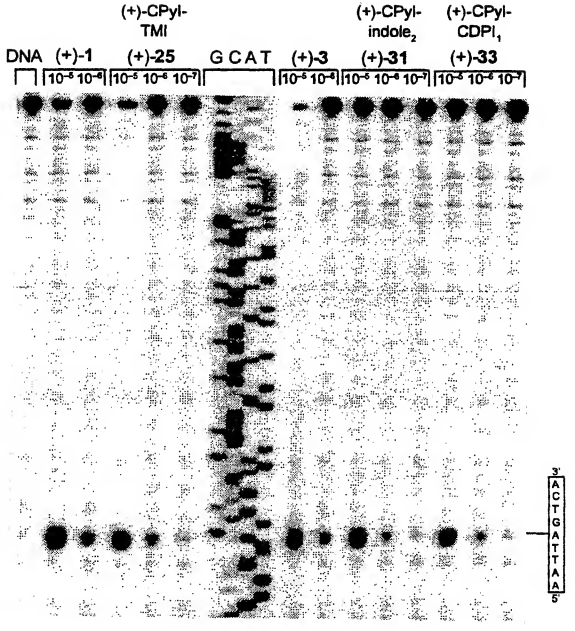
DNA
(+)-1
10⁻⁵ 10⁻⁶
(+)-CPyI-TMI
(+)-25
10⁻⁵ 10⁻⁶ 10⁻⁷
G C A T
(+)-3
10⁻⁵ 10⁻⁶
(+)-CPyI-indole2
(+)-31
10⁻⁵ 10⁻⁶ 10⁻⁷
(+)-CPyI-CDPI1
(+)-33
10⁻⁵ 10⁻⁶ 10⁻⁷
3'
A C T G A T T A A
5'

FIG. 7

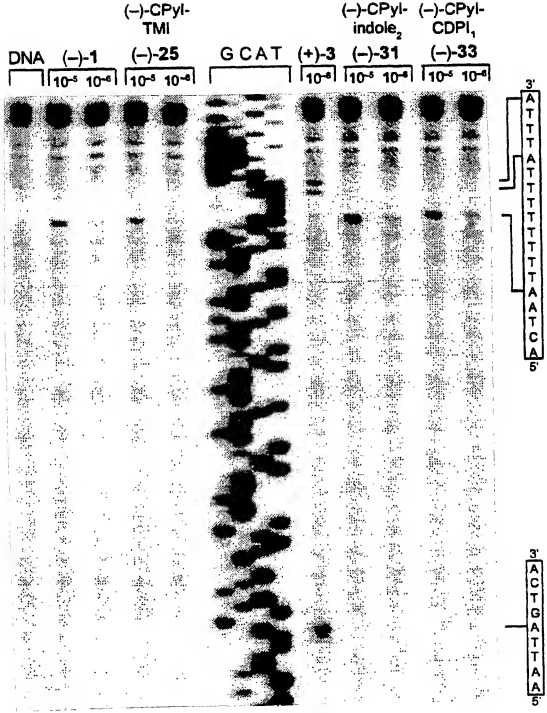
DNA
(–)-1
(–)-CPyl-TMI
(–)-25
G C A T
(+)-3
(–)-CPyl-indole2
(–)-31
(–)-CPyl-CDPI1
(–)-33
10-5 10-6
3'
ATTTATTTTTTTTAATCA
5'
3'
ACTGATTAA
5'

FIG. 8

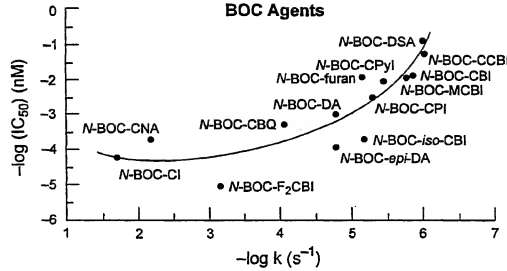
BOC Agents
N-BOC-DSA
N-BOC-CCBI
N-BOC-CPyl
N-BOC-furan
N-BOC-CBI
N-BOC-MCBI
N-BOC-DA
N-BOC-CPI
N-BOC-CBQ
N-BOC-CNA
N-BOC-iso-CBI
N-BOC-epi-DA
N-BOC-Cl
N-BOC-F2CBI
–log (IC50) (nM)
–log k (s–1)

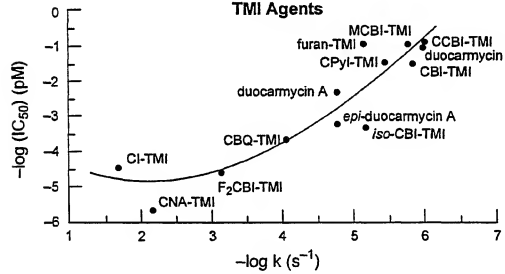
TMI Agents
MCBI-TMI
furan-TMI
CCBI-TMI
duocarmycin SA
CPyl-TMI
CBI-TMI
duocarmycin A
epi-duocarmycin A
iso-CBI-TMI
CBQ-TMI
Cl-TMI
F2CBI-TMI
CNA-TMI
–log (IC50) (pM)
–log k (s–1)

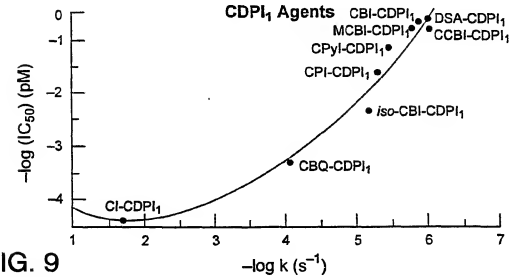
CDPI1 Agents
CBI-CDPI1
DSA-CDPI1
MCBI-CDPI1
CCBI-CDPI1
CPyl-CDPI1
CPI-CDPI1
iso-CBI-CDPI1
CBQ-CDPI1
Cl-CDPI1
–log (IC50) (pM)
–log k (s–1)

FIG. 9

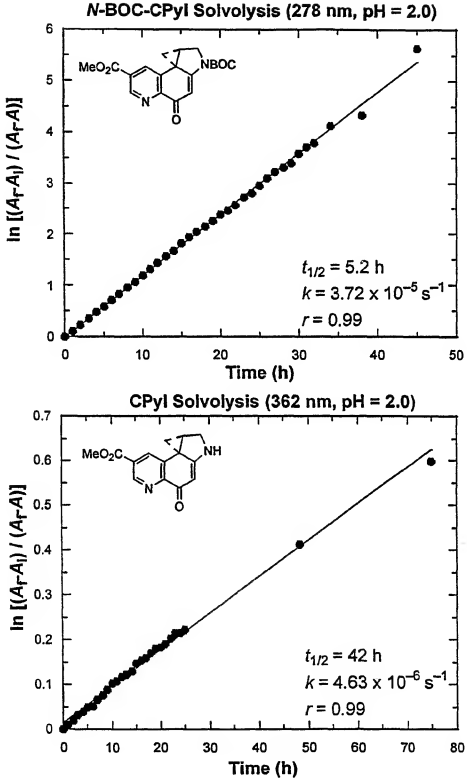
N-BOC-CPyl Solvolysis (278 nm, pH = 2.0)
MeO2C
NBOC
N
O
ln [(Af-At) / (Af-A)]
t1/2 = 5.2 h
k = 3.72 x 10−5 s−1
r = 0.99
Time (h)
CPyl Solvolysis (362 nm, pH = 2.0)
MeO2C
NH
N
O
ln [(Af-At) / (Af-A)]
t1/2 = 42 h
k = 4.63 x 10−6 s−1
r = 0.99
Time (h)

FIG. 10

Metal-Catalyzed Addition to *N*-BOC-CPyI[a]

metal	equiv	k_{obs} (s^{-1})	$t_{1/2}$ (h)
$Cu(acac)_2$	1.0	5.57×10^{-5}	3.5
$Ni(acac)_2$	1.0	3.51×10^{-5}	5.5
$Zn(acac)_2$	1.0	1.67×10^{-5}	11.5
$Cr(acac)_3$	1.0	9.73×10^{-6}	20
$Fe(acac)_3$	1.0	4.09×10^{-6}	47
$Mn(acac)_2$	1.0	9.79×10^{-7}	200
$Mg(acac)_2$	1.0	$< 7 \times 10^{-7}$	>250
none	none	stable	stable

[a] Reaction run in CH_3OH (25 °C) with addition of CH_3OH to least substituted carbon of cyclopropane (regioselectivity >40:1).

FIG. 11

Metal Cation Effect on the DNA Alkylation Efficiency of 16[a]

metal	equiv	alkylation conc (M)	efficiency enhancement
none	none	10^{-2}	–
$Cu(acac)_2$	1	10^{-2}–10^{-3}	5×
$Cu(acac)_2$	10	10^{-3}	10×
$Cu(acac)_2$	1000	10^{-4} (weak)	10–100×
$Ni(acac)_2$	10	10^{-3}	10×
$Ni(acac)_2$	1000	10^{-4}	100×
$Ni(acac)_2$	10000	10^{-5} (weak)	100–1000×
$Zn(acac)_2$	1	10^{-3}	10×
$Zn(acac)_2$	10	10^{-4}	100×
$Zn(acac)_2$	1000	10^{-5}	1000×

[a] w794 DNA, concentration of **16** at which DNA alkylation was detected (24 h, 25 °C)

FIG. 12

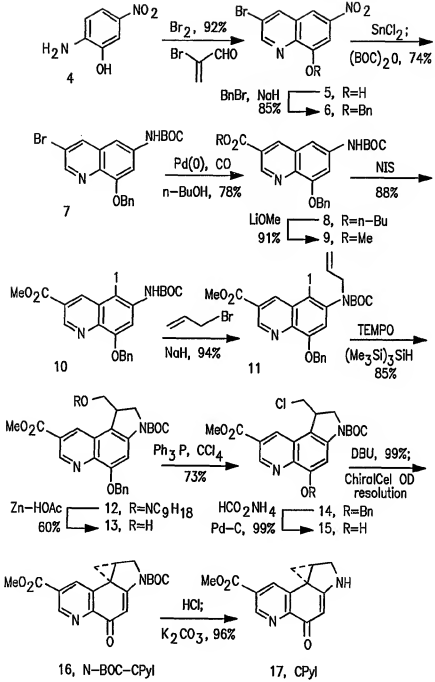
Br2, 92%
SnCl2;
(BOC)2O, 74%
BnBr, NaH
85%
5, R=H
6, R=Bn
Pd(0), CO
n-BuOH, 78%
NIS
88%
LiOMe
91%
8, R=n-Bu
9, R=Me
NaH, 94%
TEMPO
(Me3Si)3SiH
85%
Ph3P, CCl4
73%
DBU, 99%;
ChiralCel OD
resolution
Zn-HOAc
60%
12, R=NC9H18
13, R=H
HCO2NH4
Pd-C, 99%
14, R=Bn
15, R=H
HCl;
K2CO3, 96%
16, N-BOC-CPyl
17, CPyl

FIG. 13

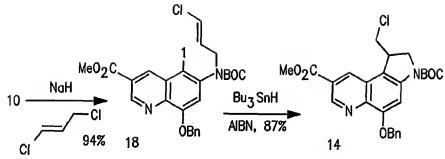
Cl
1
MeO2C
NBOC
10
NaH
Cl
Cl
94%
18
N
OBn
Bu3SnH
AIBN, 87%
Cl
MeO2C
NBOC
N
OBn
14

FIG. 14

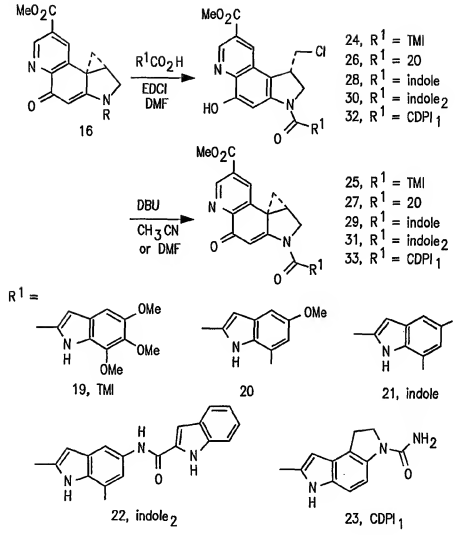
MeO2C
R1CO2H
EDCI
DMF
16
24, R1 = TMI
26, R1 = 20
28, R1 = indole
30, R1 = indole2
32, R1 = CDPI1
DBU
CH3CN
or DMF
25, R1 = TMI
27, R1 = 20
29, R1 = indole
31, R1 = indole2
33, R1 = CDPI1
R1 =
19, TMI
20
21, indole
22, indole2
23, CDPI1

FIG. 15

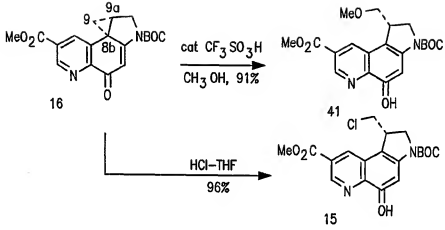
9a
9
8b
MeO2C
NBOC
N
O
16
cat CF3SO3H
CH3OH, 91%
MeO
MeO2C
NBOC
N
OH
41
HCl–THF
96%
Cl
MeO2C
NBOC
N
OH
15

FIG. 16

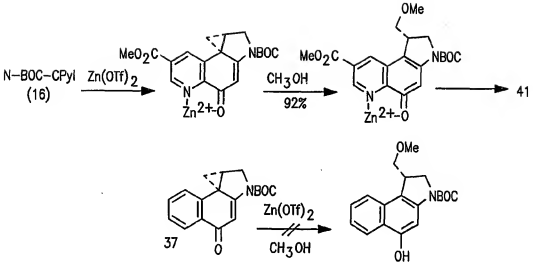

FIG. 17

Solvolysis Rates with Phosphate Buffer [a]

compd		$k_{obs}(S^{-1})$	$t_{1/2}$(h)
16. n-BOC-CPyI	pH 2	3.72×10^{-5}	5
	pH 3	3.81×10^{-6}	51
17. CPyI	pH 2	4.63×10^{-6}	42
	pH 3	6.27×10^{-7}	310

[a] pH 2: 50% CH_3OH–aqueous buffer (4:1:20 (v:v:v) 1.0 M citric acid. 0.2 M Na_2HPO_4, and H_2O, respectively. pH 3: 50% CH_3OH–aqueous buffer (4:1:20 (v:v:v) 0.1 M citric acid, 0.2 M Na_2HPO_4, and H_2O, respectively).

FIG. 18

Solvolysis Rates of N-BOC-CPyI with Universal Buffer [a]

pH	k_{abs} (S^{-1})	$t_{1/2}$ (h)
2.0	3.45×10^{-5}	5.5
3.0	4.79×10^{-6}	40
4.0	1.15×10^{-6}	165
5.0	8.41×10^{-7}	230
6.0	7.88×10^{-7}	245
7.0	8.29×10^{-7}	230
8.0	7.27×10^{-7}	265
9.0	6.73×10^{-7}	290
10.0	6.97×10^{-7}	275
50% CH_3OH-H_2O	9.80×10^{-7}	195
CH_3OH	stable	stable

[a] 50% CH_3OH-aqueous buffer ($B(OH)_3$-citric acid-Na_3PO_4).

FIG. 19

in Vitro Cytotoxic Activity

agent	configuration	IC_{50} (L1210) [a]
16. (+)-N-BOC-CPyI	natural	110 nM
16. (-)-N-BOC-CPyI	unnatural	70 nM
17. (+)-CPyI	natural	1 μM
17. (-)-CPyI	unnatural	2 μM
25. (+)-CPyI-TMI	natural	27 pM (21 pM)
25. (-)-CPyI-TMI	unnatural	850 pM (350 pM)
27. (+)-27	natural	30 pM (40 pM)
27. (-)-27	unnatural	500 pM (500 pM)
29. (+)-CPyI-indole	natural	400 pM (800 pM)
29. (-)-CPyI-indole	unnatural	1000 pM (800 pM)
31. (+)-CPyI-indole$_2$	natural	8 pM (7 pM)
31. (-)-CPyI-indole$_2$	unnatural	45 pM (30 pM)
33. (+)-CPyI-CDPI$_1$	natural	15 pM (10 pM)
33. (-)-CPyI-CDPI$_1$	unnatural	40 pM (30 pM)

[a] The value in parentheses corresponds to the IC_{50} value determined for the corresponding seco precursor.

FIG. 20

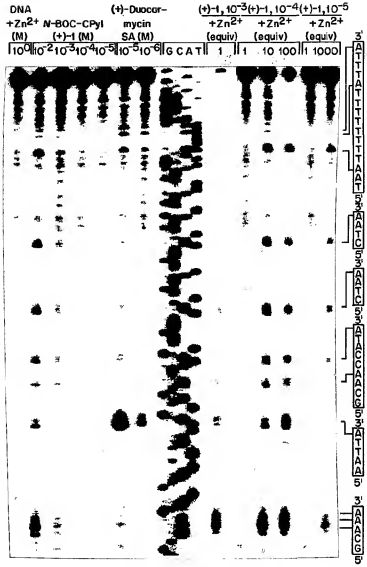

Thermally induced strand cleavage of w794 DNA (SV40 DNA segment, 144 bp, nucleotide nos. 138-5238): DNA-agent incubation for 24 h at 25 C, removal of unbound agent and 30 min of thermolysis (100 C), followed by denaturing 8% PAGE and autoradiography: lane 1, control DNA with $Zn(acac)_2$ (1 M); lanes 2-5. (+)-*N*-BOC-CPyI (1, 1 x 10^{-2} to 1 M); lanes 6-7. (+)-duocarmycin SA (1 x 10^{-5} and 1 x 10^{-6} M): lanes 8-11, Sanger G. C. A. and T sequencing reactions; lane 12, (+)-*N*-BOC-CPyI (**1**, 1 x 10-3 M) with $Zn(acac)_2$ (1, 10, and 100 equiv): lanes 16-17, (+)-*N*-BOC-CPyI (**1**, 1 x 10^{-3} M) with $Zn(acac)_2$ (1 and 1000 equiv). Note: In lanes containing extensive DNA cleavage, the greater intensity of the shorter oligonucleotide cleavage sites observed at the lower half of the gel is a consequence of multiple cleavages producing greater proportions of the short fragments and do not represent a change in the alkylation selectivity.

FIG. 21

INTERNATIONAL SEARCH REPORT

International application No.
PCT/US01/14374

A. CLASSIFICATION OF SUBJECT MATTER
IPC(7) : C07D 471/04, 471/08, 487/04, 487/08; C07F 1/08, 1/10, 3/06, 11/11, 15/02.
US CL. : 546/70,84,3,8,9
According to International Patent Classification (IPC) or to both national classification and IPC

B. FIELDS SEARCHED
Minimum documentation searched (classification system followed by classification symbols)
U.S. : 546/3, 8,9,70,84

Documentation searched other than minimum documentation to the extent that such documents are included in the fields searched

Electronic data base consulted during the international search (name of data base and, where practicable, search terms used)

C. DOCUMENTS CONSIDERED TO BE RELEVANT

Category *	Citation of document, with indication, where appropriate, of the relevant passages	Relevant to claim No.
X	WO 99/29642 A (THE SRIPPS RESEARCH INSTITUTE) 17 June 1999 ,see entire document	3,4, 10 and 12
Y	US 4,912,227 A (KELLY et al) 27 MARCH 1990 see entire document.	1-18

☐ Further documents are listed in the continuation of Box C. ☐ See patent family annex.

* Special categories of cited documents:

"A" document defining the general state of the art which is not considered to be of particular relevance

"E" earlier application or patent published on or after the international filing date

"L" document which may throw doubts on priority claim(s) or which is cited to establish the publication date of another citation or other special reason (as specified)

"O" document referring to an oral disclosure, use, exhibition or other means

"P" document published prior to the international filing date but later than the priority date claimed

"T" later document published after the international filing date or priority date and not in conflict with the application but cited to understand the principle or theory underlying the invention

"X" document of particular relevance; the claimed invention cannot be considered novel or cannot be considered to involve an inventive step when the document is taken alone

"Y" document of particular relevance; the claimed invention cannot be considered to involve an inventive step when the document is combined with one or more other such documents, such combination being obvious to a person skilled in the art

"&" document member of the same patent family

Date of the actual completion of the international search	Date of mailing of the international search report
	24 AUG 2001
Name and mailing address of the ISA/US Commissioner of Patents and Trademarks Box PCT Washington, D.C. 20231 Facsimile No. (703)305-3230	Authorized officer Alan L. Rotman Telephone No. 703-308-0193

Form PCT/ISA/210 (second sheet) (July 1998)